

AD-A047 385

PHYSICS INTERNATIONAL CO SAN LEANDRO CALIF
APPLICATION OF FAE TECHNOLOGY TO THE DESIGN OF NUCLEAR AIRBLAST--ETC(U)
AUG 77 F SAUER, T STUBBS
PIFR-978

UNCLASSIFIED

DNA-4327F

F/6 19/4
DNA001-76-C-0354
NL

| OF |
AD
A047385



END
DATE
FILMED
1-78
DDC

AD A 0 47 385

12
MS

AD-E300025

DNA 4327F

APPLICATION OF FAE TECHNOLOGY TO THE DESIGN OF NUCLEAR AIRBLAST SIMULATION EXPERIMENTS

Physics International Company
2700 Merced Street
San Leandro, California 94577

August 1977

Final Report for Period September 1976—February 1977

CONTRACT No. DNA 001-76-C-0354

APPROVED FOR PUBLIC RELEASE;
DISTRIBUTION UNLIMITED.

THIS WORK SPONSORED BY THE DEFENSE NUCLEAR AGENCY
UNDER RDT&E RMSS CODE B3407T464 Y99QAXSD07025 H2590D.

Prepared for
Director
DEFENSE NUCLEAR AGENCY
Washington, D. C. 20305

DDC
RECEIVED
DEC 12 1977
B

DDC FILE COPY

Destroy this report when it is no longer
needed. Do not return to sender.



UNCLASSIFIED

SECURITY CLASSIFICATION OF THIS PAGE (When Data Entered)

REPORT DOCUMENTATION PAGE		READ INSTRUCTIONS BEFORE COMPLETING FORM
1. REPORT NUMBER DNA 4327F	2. GOVT ACCESSION NO.	3. RECIPIENT'S CATALOG NUMBER
4. TITLE (and Subtitle) APPLICATION OF FAE TECHNOLOGY TO THE DESIGN OF NUCLEAR AIRBLAST SIMULATION EXPERIMENTS.	5. TYPE OF REPORT	6. PERIOD COVERED Final Report, for period Sep 76 - Feb 77
7. AUTHOR(s) F./Sauer T./Stubbs	8. PERFORMING ORG. REPORT NUMBER PIFR-978	9. CONTRACT OR GRANT NUMBER(s) DNA 001-76-C-0354
9. PERFORMING ORGANIZATION NAME AND ADDRESS Physics International Company 2700 Merced Street San Leandro, California 94577	10. PROGRAM ELEMENT, PROJECT, TASK AREA & WORK UNIT NUMBERS Subtask Y99QAXSD070-25	
11. CONTROLLING OFFICE NAME AND ADDRESS Director Defense Nuclear Agency Washington, D.C. 20305	12. REPORT DATE August 1977	13. NUMBER OF PAGES 68
14. MONITORING AGENCY NAME & ADDRESS (if different from Controlling Office) 1264p.	15. SECURITY CLASS (of this report) UNCLASSIFIED	15a. DECLASSIFICATION DOWNGRADING SCHEDULE
16. DISTRIBUTION STATEMENT (of this Report) Approved for public release; distribution unlimited 18 DNA, SBIE 19 4327F, AD-E300 025		
17. DISTRIBUTION STATEMENT (of the abstract entered in Block 20, if different from Report)		
18. SUPPLEMENTARY NOTES This work sponsored by the Defense Nuclear Agency under RDT&E RMSS Code B3407T464 Y99QAXSD07025 H2590D.		
19. KEY WORDS (Continue on reverse side if necessary and identify by block number) Fuel-Air-Explosives Nozzle Performance Nuclear Airblast Simulation Fuel Costs Airblast Nuclear Equivalency FAE Detonability FAX		
20. ABSTRACT (Continue on reverse side if necessary and identify by block number) The detonation of fuel aerosols and vapors in air is investi- gated with respect to the applicability of this type of explosion to generating an airblast simulation a 1-KT nuclear airburst ex- plosion. Extensive investigations into existing overpressure and overpressure-impulse data from weaponized FAE's and carefully controlled hemispherical balloon detonations has allowed a comparison of the fuel-air explosives with both condensed ex- plosives (TNT and nitromethane) and a predicted 1-KT nuclear		

282 760

LB

UNCLASSIFIED

SECURITY CLASSIFICATION OF THIS PAGE(When Data Entered)

20. ABSTRACT (Continued).

surface burst. It was found that, depending upon cloud geometry, the total fuel required for a 1-KT nuclear airblast simulation varied between 63 and 200 tons. The concentration of fuel in air must be close to stoichiometric and the mean droplet diameter must be 2500 microns or less.

Investigation into existing nozzles indicate that it is questionable whether commercially available nozzles can project a vapor to the requisite height for the 1-KT simulation.

Various fuel candidates were investigated. We found that the prop-hydrocarbon compounds are attractive with higher order hydrocarbons being worth consideration.

ACCESSION for	
NTIS	White Section <input checked="" type="checkbox"/>
DOC	Buff Section <input type="checkbox"/>
RTI/ANNOUNCED	<input type="checkbox"/>
JUSTIFICATION	
BY	
DISTRIBUTION/AVAILABILITY CODES	
Dist	and/or SPECIAL
A	

UNCLASSIFIED

SECURITY CLASSIFICATION OF THIS PAGE(When Data Entered)

CONTENTS

<u>SECTION</u>		<u>PAGE</u>
1	INTRODUCTION	5
2	PROGRAM OBJECTIVES	9
3	COMPARISONS OF FAE AIRBLAST DATA WITH NUCLEAR HIGH EXPLOSIVE DATA	11
	3.1 Condensed High Explosive Airblast Data	11
	3.2 Explosively Disseminated Fuel Clouds	15
	3.3 Hemispherical Balloons Filled with Fuel-Air Mixtures	25
	3.4 Summary	27
4	EFFECT OF CLOUD GEOMETRY AND WIND ON SIMULATION EXPERIMENT DESIGN	32
5	DETONABILITY OF AEROSOL-AIR MIXTURES	37
6	SPRAY NOZZLE TECHNOLOGY REVIEW	43
	6.1 Nozzle Performance	43
	6.2 Theoretical Vertical Reach	49
	6.3 Summary	53
7	COMPARISON OF CANDIDATE FUELS	54
8	CONCLUSIONS AND RECOMMENDATIONS	58
	REFERENCES	60

ILLUSTRATIONS

<u>FIGURE</u>		<u>PAGE</u>
1	Scaled Overpressure for TNT and Nitromethane Tangent-to-the-Surface Spheres Compared with Overpressure from a 1-KT Nuclear Surface Burst	12
2	Scaled Overpressure Impulse for TNT and Nitromethane Tangent-to-the Surface Spheres Compared with Impulse from a 1-KT Nuclear Surface Burst	13
3	Typical Overpressure Waveforms from Static FAE Warhead Detonations at NWC, China Lake, CA	16
4	Measured Cloud Diameter as a Function of Time for Nominal 1400 Pound FAE Warheads	19
5	Measured Cloud Height as a Function of Time for Nominal 1400 Pound FAE Warheads	20
6	Scaled Overpressure for Ethylene Oxide FAE Compared with Overpressure from a 1-KT Nuclear Surface Burst	21
7	Scaled Overpressure Impulse for Ethylene Oxide FAE Compared with Impulse from a 1-KT Nuclear Surface Burst	22
8	Scaled Overpressure Impulse for BLU-73/B Warheads Compared with Impulse from a 1-KT Nuclear Surface Burst	24
9	Scaled Overpressures for MAPP-Air Explosions Compared with Overpressure from a 1-KT Nuclear Surface Burst	28

Illustrations (Continued)

<u>FIGURE</u>		<u>PAGE</u>
10	Scaled Overpressure-Impulse for MAPP-Air Explosions Compared with Impulse from 1-KT Nuclear Surface Burst	29
11	Scaled Overpressure-Impulse for Propane-Oxygen Explosions Compared with Impulse from 1-KT Nuclear Surface Burst	30
12	Calculated Overpressure Impulse as a Function of Overpressure Scaled to Source Energy of 10^{12} cal (1-KT)	33
13	Error in Predicted Overpressure Due to Cloud Translation by Wind	35
14	Critical Threshold Energy for Detonation Initiation as a Function of MAPP Concentration in Air	39
15	Spray Detonation Velocity for Kerosene 2 as a Function of Equivalence Ratio and Drop Size	40
16	Comparison of Experimental Detonation Velocity with the Ideal CJ Velocity	41
17	Spray Particle Size Versus Pressure	46
18	Mean Drop Diameter Versus Flow Rate and Pressure Drop Across Nozzle	47

SECTION 1

INTRODUCTION

A continuing responsibility of the Defense Nuclear Agency (DNA) is to provide nuclear weapon effects simulation facilities to the Services in support of service requirements to test and certify various equipments against the nuclear environment. As part of this program, large high explosive events simulating the airblast from approximately a 1 KT nuclear detonation have been fielded on an average of one per year since the Snowball event in 1964 (if one accounts for some years with up to three detonations, e.g., the Sailor Hat series). All large simulation events (not counting the relatively small 20 ton gaseous mixture events) have utilized condensed explosives (TNT, ANFO, or nitromethane) as the explosive source, either as a matter of convenience or historical precedence, e.g., the use of recast, surplus TNT, because a cratering event was also a simulation requirement, e.g., Pre-Dice Throw and Pre-Mine Throw IV, or because no suitable alternative was available, e.g., Dice Throw.

For simulation events whose primary purpose is to provide an airblast environment, the cratering aspects of condensed explosives placed directly on the ground surface are detrimental in that the crater ejecta may cause unwanted impacts on airblast targets and the crater needs refilling and extensive rehabilitation of the test bed is required before a test may be repeated using the same ground zero. Since gage mounts, cabling, trenching, instrument power and like capital investments represent a

considerable fraction of the cost of a large simulation test, the cost savings of a reusable test facility could be substantial. Also for most systems where airblast is the primary damage mechanism, e.g., for tactical land-based systems, the high airblast overpressures produced by condensed (solid) explosives are unnecessary for nuclear simulation purposes.

These requirements to conduct frequent tests of various military equipment against the simulated airblast from nuclear weapons have emphasized the desirability of a reusable facility for such purposes. In a reusable facility, airblast gage mounts, instrumentation, cabling, and other test-bed hardware would be permanently emplaced, resulting in decreased costs of testing and decreased turn-around time. The nuclear airblast simulation technique employed in the facility should be able to generate highly uniform and repeatable overpressure and dynamic pressure waveforms consistent with the waveforms from a 1-KT nuclear surface burst for overpressures from approximately 1 psi to 100 psi. In certain research applications, the ability to vary the equivalent nuclear yield easily would be advantageous.

Detonable gas mixtures contained in balloons for the purpose of nuclear-airblast simulation have received considerable attention by DNA (Reference 1). Properly mixed mixtures of methane/oxygen and propane/oxygen produce clean, reproducible airblast waves and their low detonation pressures (~ 600 psi) preclude disturbance of the test bed. These would seem ideal for airblast simulation purposes except for the long filling times of the large (~ 300-foot diameter) hemispheres, their susceptibility to wind loads, the high cost of the balloons, and the safety aspects of handling detonable gas mixtures.

However, the success of the detonable-gas balloon concept in simulating low yield (~ 20 ton) nuclear detonations argues in favor of the concept that free air, i.e., without balloon confinement fuel-air explosions (FAE) could provide an adequate simulation of a 1-KT nuclear explosion without the complications, cost, fill time and safety aspects of the detonable-gas balloon. In addition fuel-air explosions have been successfully adapted as a military airblast-effects weapon, e.g., the BLU-73/B, and devices containing up to 1400 pounds of explosively-disseminated fuel (ethylene oxide) have been successfully detonated (Reference 2). These devices give airblast pulses similar to those obtained from other high explosives and/or nuclear detonations.

Theoretical analysis (Reference 3) of the energetics of FAE leads to the conclusion that these detonations may be five to ten times as effective per unit weight (including only the weight of the fuel as the explosive) as condensed explosives in producing airblast since the FAE rely on the atmosphere for its oxidizer. Cost comparisons of raw explosive, based on somewhat uncertain TNT equivalences, are favorable for FAE fuels, e.g., ethylene oxide appears to be one-half the cost of ANFO per pound of TNT equivalent. Consequently, FAE have also the potential of being considerably more cost-effective than condensed explosives for nuclear airblast simulation.

The volumes occupied by stoichiometric FAE mixtures are, however, approximately four times larger than those for methane-oxygen mixtures and hence it appears that the single most important question related to FAE as a practical airblast simulation concept is whether or not uniform, repeatable mixing of the fuel with the air can be routinely achieved on a time scale of

a few seconds or tens of seconds. It should be noted that even balloons containing detonable gases are not automatically well behaved and that a considerable effort was expended to assure complete mixing of, for example, methane and oxygen before repeatable and reproducible detonations were obtained (see Figures 4.121 and 4.122 of Reference 4). Complete mixing is even more of a requirement for fuel-air mixtures as evidenced by the much greater sensitivity of detonation pressures on the mixture ratio of oxidizer and fuel when using air versus using oxygen (see, for example, Figure 2.47 of Reference 4).

SECTION 2

PROGRAM OBJECTIVES

To be cost-effective, a nuclear airblast simulation technique must be azimuthally uniform (or predictably non-uniform) and, within limits, repeatable in its overpressure and overpressure-impulse versus distance relationships. Otherwise critical experiments may not experience the desired loadings and/or certification tests may be invalidated for the same reason. Even condensed explosive sources have a problem area in this respect at high overpressures due to jetting and airblast "anomalies" observed for certain source geometries.

Airblast data from statically fired FAE experiments, especially data from the larger charge sizes, provides a basis for estimating the degree of reproducibility associated with FAE and, when compared with nuclear overpressure data, these data also give experimentally based estimates of the nuclear simulation efficiency of FAE. The first objective of the current study was to review and document the pertinent FAE data and make comparisons with high explosive, nuclear-airblast simulation data and nuclear-airblast data.

Because of the large volume associated with stoichiometric fuel-air mixtures, e.g., $1.5 \times 10^6 \text{ m}^3$ for an energy release of 1 kt (4.10^{12} joules) or a hemisphere 90 meters in radius, successful fuel-dispersal methods are believed to be the kernel of a

successful FAE nuclear airblast simulation. Large amounts of fuel must be dispersed uniformly in a very short time. Due to high dynamic pressure impulses within the FAE fireball, structures to support fuel dispersal equipment do not appear cost-effective or desirable. As an alternate to in-cloud dispersal point systems, ground-based nozzles were recommended as a primary method of dispersal (Reference 3). Since data on commercial nozzle characteristics (such as flow volume, spray angle, reach, and droplet size) necessary to demonstrate the feasibility of a ground-based nozzle system were not documented in previous studies (References 3 and 5), the second objective of the study was to document and analyze these data.

SECTION 3

COMPARISONS OF FAE AIRBLAST DATA WITH NUCLEAR HIGH EXPLOSIVE DATA

As the objective of a nuclear airblast simulation program is to simulate a 1-KT nuclear surface-burst, all data will be compared on that basis. The standard nuclear surface burst curve of overpressure versus distance is given in the Figure 4.3-51 of Reference 6. This curve is a composite of all maximum overpressure data recorded on nuclear surface bursts. The mean curve to the data has been fitted statistically and maximum data scatter about the mean is ± 13 percent. The curve of overpressure impulse as a function of overpressure was constructed using Figure 4.3-51 of Reference 6 and Figure 4.3-57 which shows a scatter of ± 30 percent for overpressure impulse about the mean value at a given range. In making the comparison with high explosive and FAE airblast, the nuclear data will be presented with the nuclear data scatter shown as shaded bands.

3.1 CONDENSED HIGH EXPLOSIVE AIRBLAST DATA

Before presenting the FAE airblast data, it is worthwhile to assess data from nuclear-airblast simulation events using condensed high explosives. Figures 1 and 2 present data from five surface-tangent spheres of TNT (Reference 7) and two surface-tangent spheres of nitromethane (Reference 8). Because of the nature of the high explosive source, i.e., the tangent-to-the-surface geometry, overpressures above 10 psi are larger

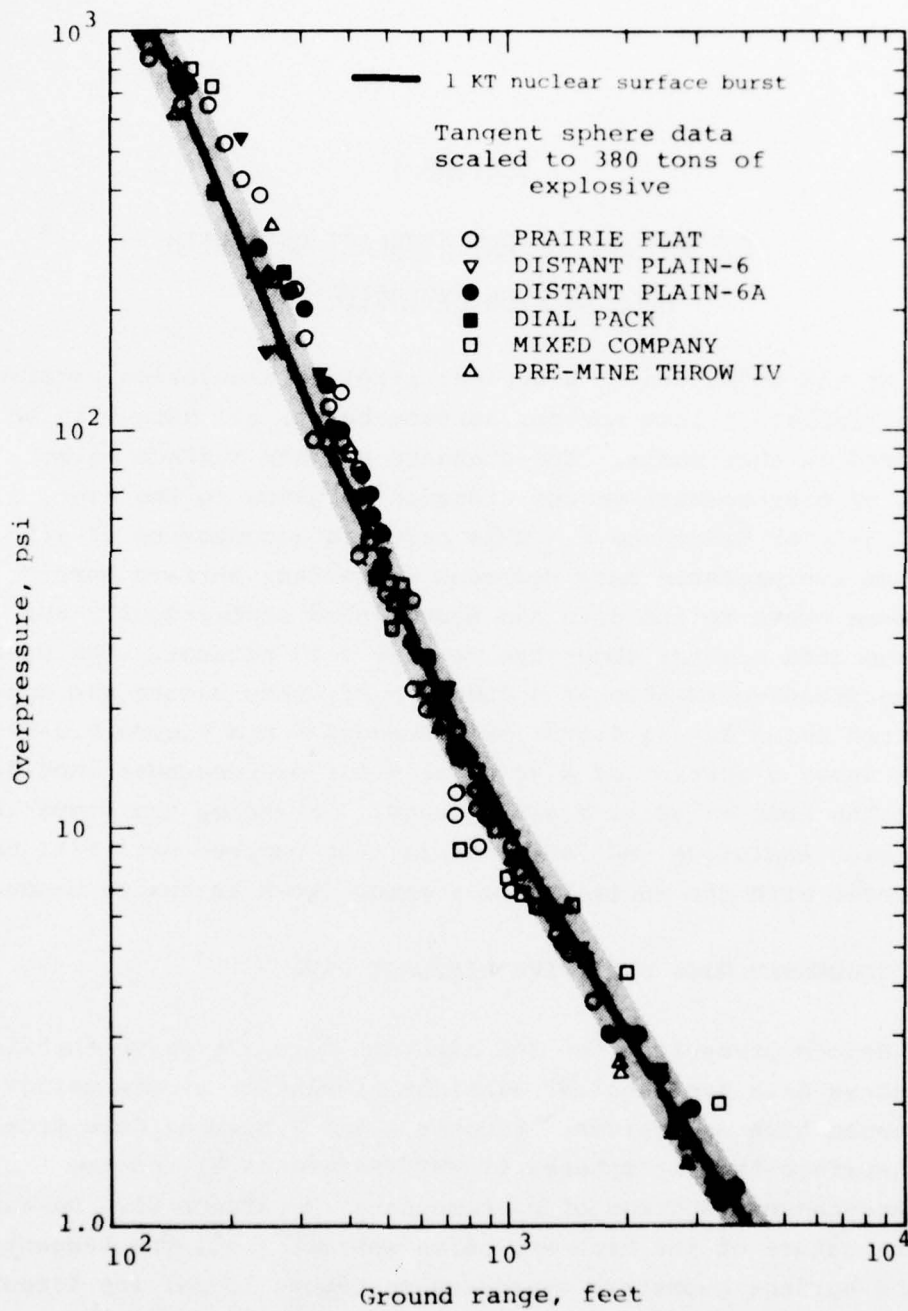


Figure 1 Scaled overpressure for TNT and nitromethane tangent-to-the-surface spheres compared with overpressure from a 1 KT nuclear surface burst (shaded area shows scatter of nuclear data).

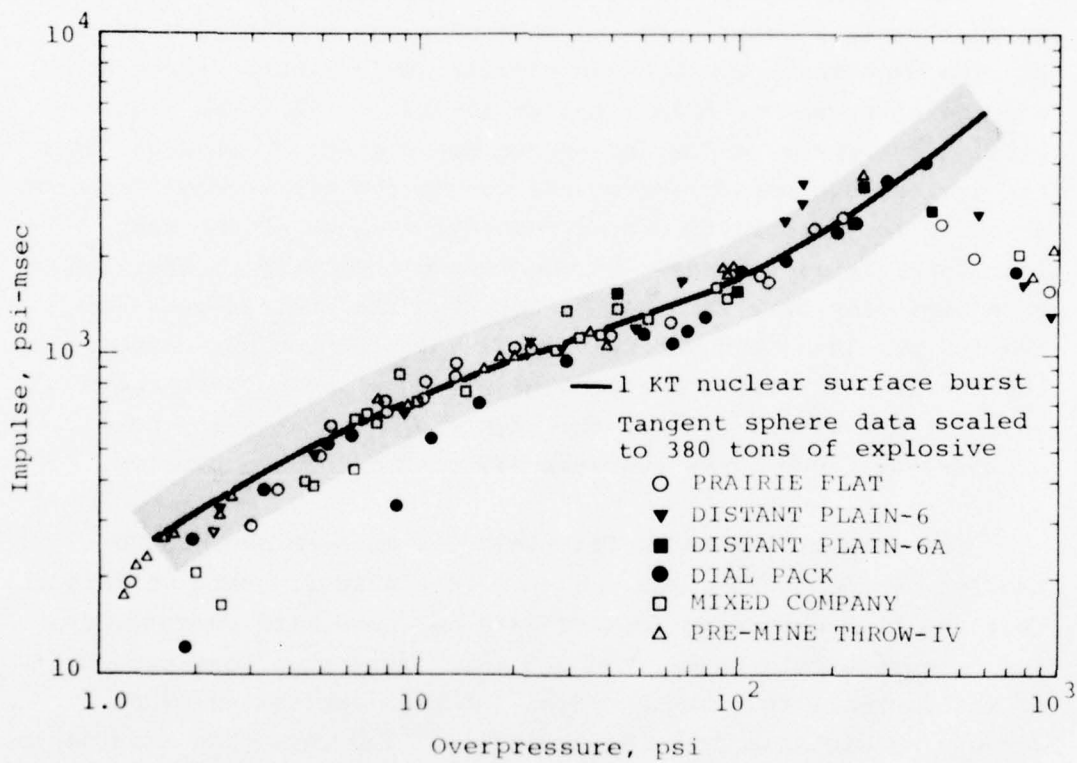


Figure 2 Scaled overpressure impulse for TNT and nitromethane tangent-to-the-surface spheres compared with impulse from a 1 KT nuclear surface burst (shaded area shows scatter of nuclear data).

than those for the equivalent weight hemisphere. The data have been corrected to the same standard conditions of temperature and pressure (STP) as used for the standard nuclear surface-burst curve.

The overpressure versus ground range data were "fit" to the nuclear surface-burst curve to determine the weight of high explosive necessary to match the nuclear surface-burst curve over a range of pressures from 1 psi to 100 psi. Since the high explosive overpressure-distance curve has a greater curvature than the nuclear overpressure-distance curve, the two sets of data can never be in juxtaposition over the entire range of interest. Therefore, it is necessary to compromise the "fit" to have the high explosive data somewhat higher than the nuclear curve at the 100 psi level and somewhat lower than the nuclear curve at the 10 psi level and approximately equal to nuclear curve at the 1 psi level. To fit the high explosive data to the nuclear pressure-distance curve requires 380 tons of high explosive.

The same procedure in "fitting" the nuclear overpressure impulse-overpressure curve was used in Figure 2. Here we note that the high explosive impulse data decrease with overpressure for overpressure greater than 300 psi. This is a consequence of the decrease in pulse duration for high explosives with decreasing distance from the explosion. The three low impulse points on Dial Pack and the two low impulse points on Mixed Company are undoubtedly the results of airblast anomalies which frequently accompany the surface-tangent sphere charge configuration. The same 380 tons of high explosive are required to match the nuclear curve; in fact, in matching the nuclear curves of Figure 1 and 2, consistency in the yield equivalency of the high explosive was an overriding factor in the "fitting" of the high explosive to the nuclear data.

It should be noted that it is the overpressure impulse-overpressure relationship which is most important in determining the fuel efficiency relative to a nuclear detonation since the testing of equipment depends more on having the proper impulse at the desired overpressure rather than having exactly the nuclear overpressure at a specific range from the burst point. Stated another way, the desired overpressure may be obtained by adjusting the range from the burst point, but the desired impulse at that overpressure can only be obtained by adjusting the charge weight.

The 380 tons of high explosive necessary to simulate the 1-kt nuclear airblast is significantly lower than the 500 tons of high explosive usually quoted as the nuclear-to-high-explosive equivalency. This is because the 500 ton equivalence derives from overpressure data from hemispherical charges of TNT which produce lower overpressures in the region above 10 psi (see Figure 10a of Reference 9), and that a compromise has been made in the fitting of the overpressure-range curve for the tangent sphere data.

3.2 EXPLOSIVELY DISSEMINATED FUEL CLOUDS

Airblast data from static firings of FAE warheads were obtained from References 2 and 10 and from examination of pressure gage records at the Naval Weapons Center (NWC), China Lake, California. Why the latter was necessary is illustrated in Figure 3 which presents tracings of oscillograph records of pressure gage outputs from a typical FAE warhead detonation. Immediately noticeable is the multiplicity of shock waves associated with pressure pulses exterior to the FAE fireball. The origin of the secondary and tertiary shock systems comes from the manner in which the FAE cloud was detonated. Since



Figure 3 Typical overpressure waveforms from static FAE warhead detonations at NWC, China Lake, CA. (Maximum overpressure readings indicated as read by FMS).

the explosively disseminated clouds tend to be lean in fuel at the center and rich toward the outer edges, the detonators (usually two) are placed off-center from the canister resulting in a nonsymmetrical series of detonations and collisions of shocks within the FAE cloud; the net result being a multiplicity of shocks in the airblast output of the FAE. Since the duration of airblast pulses from these warheads is short (several tens of milliseconds), the targets against which these weapons are intended to be used are generally sensitive to overpressure impulse rather than peak overpressure. Consequently the multiple shock characteristics are not generally detrimental to the performance of the warhead.

Multiple airblast shocks are, however, deleterious in a nuclear-airblast simulation system since, except in special circumstances, double shocks are not associated with nuclear airblast pulses. What makes the problem even more complicated for explosively disseminated clouds is that the double shocks are not symmetric about the center of the cloud since the detonation points have been offset from the warhead. In a practical nuclear-airblast simulation, these multiple shocks can possibly be avoided by providing a more uniform fuel distribution and centrally located cloud detonation points.

A second feature of the waveforms is the occurrence of numerous pressure spikes of extremely short duration.* In evaluating high explosive airblast data, such spikes would be edited out during data interpretation and the maximum overpressures read from the records as shown in Figure 3. Every pressure record used in the analysis of the 300-, 1000- and 1400-pound FAE warhead data was examined and maximum pressures

*The so-called "impulse-less pressures" at the NWC

reread, if necessary, to eliminate pressure spikes from the data. This procedure actually resulted in a tighter set of data, albeit somewhat lower maxima, than were reported in References 2 and 10.

The fuel clouds were approximately cylindrical in shape having a height to diameter ratio of 0.2. For the nominal 1400 pound warheads, the cloud diameter was approximately 115 feet and the cloud height approximately 23 feet. The detonators were placed at 30 and 40 feet respectively from the warhead at right angles to the pressure gage line. The clouds were detonated at approximately 370 msec after ignition of the burster. Figure 4 and 5 show the radius and height of the clouds as a function of time for several nominal 1400 pound warheads.

The data from the 300-, 1000-, and 1400-pound FAE warhead detonations were corrected to STP and scaled to a common yield by the usual one-third power-of-yield scaling rules. The data were then fitted to the nuclear surface burst curve in the same manner described for the high explosive data, i.e., matching the overpressure versus ground range curve between the 1 psi and 100 psi limits (Figure 6).

Because multiple shocks appeared to increase the duration of the waveforms, it was thought that there might be a tendency toward higher impulses for the multiple shock waveforms over a single shock system, consequently the data were sorted on this basis in Figure 7 (data points showing ticks correspond to multiple shock waveforms). There appeared to be no trend in this direction discernible within the scatter of the data, and consequently this effect was ignored in fitting the impulse versus overpressure curve against the nuclear data.

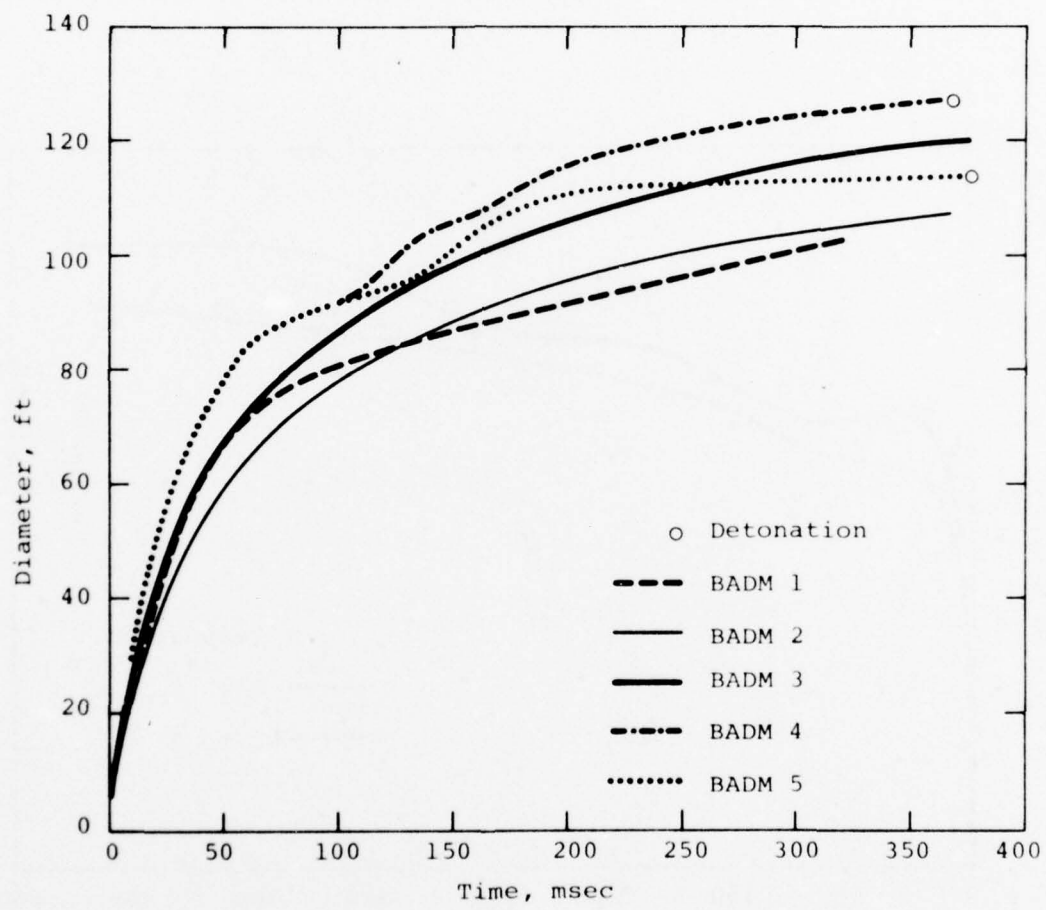


Figure 4 Measured cloud diameter as a function of time for nominal 1400 pound FAE warheads.

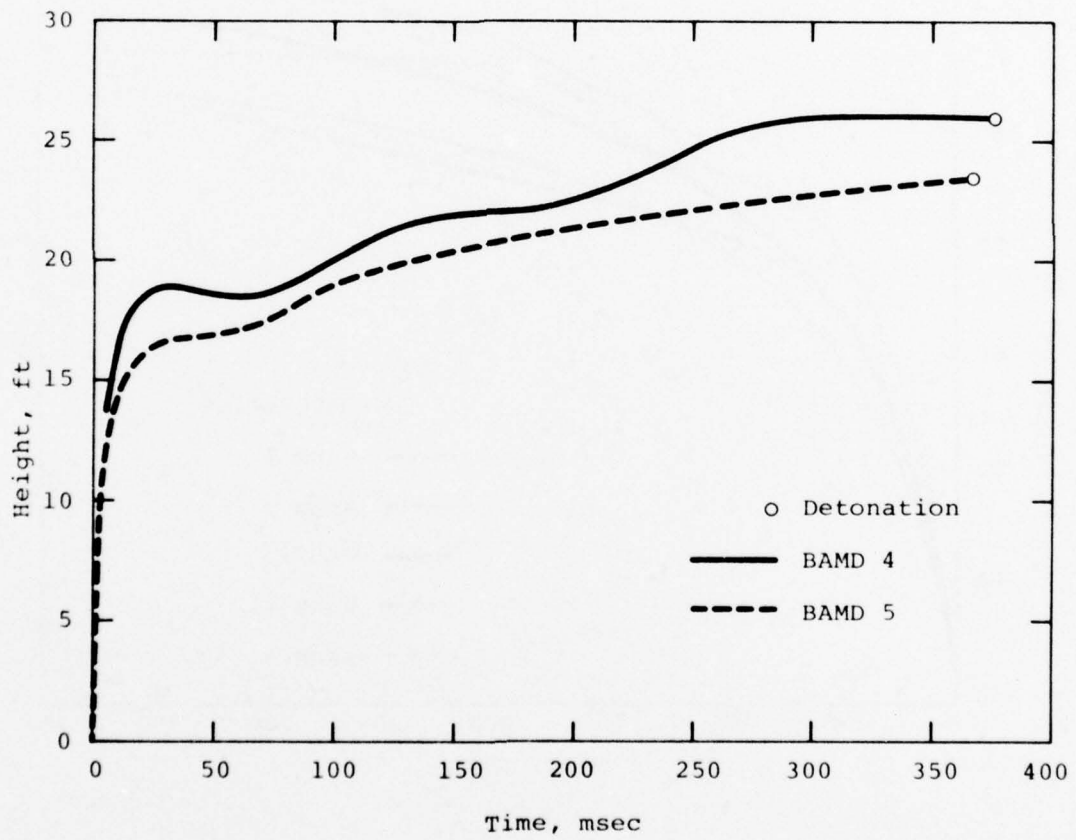


Figure 5 Measured cloud height as a function of time for nominal 1400 pound FAE warheads.

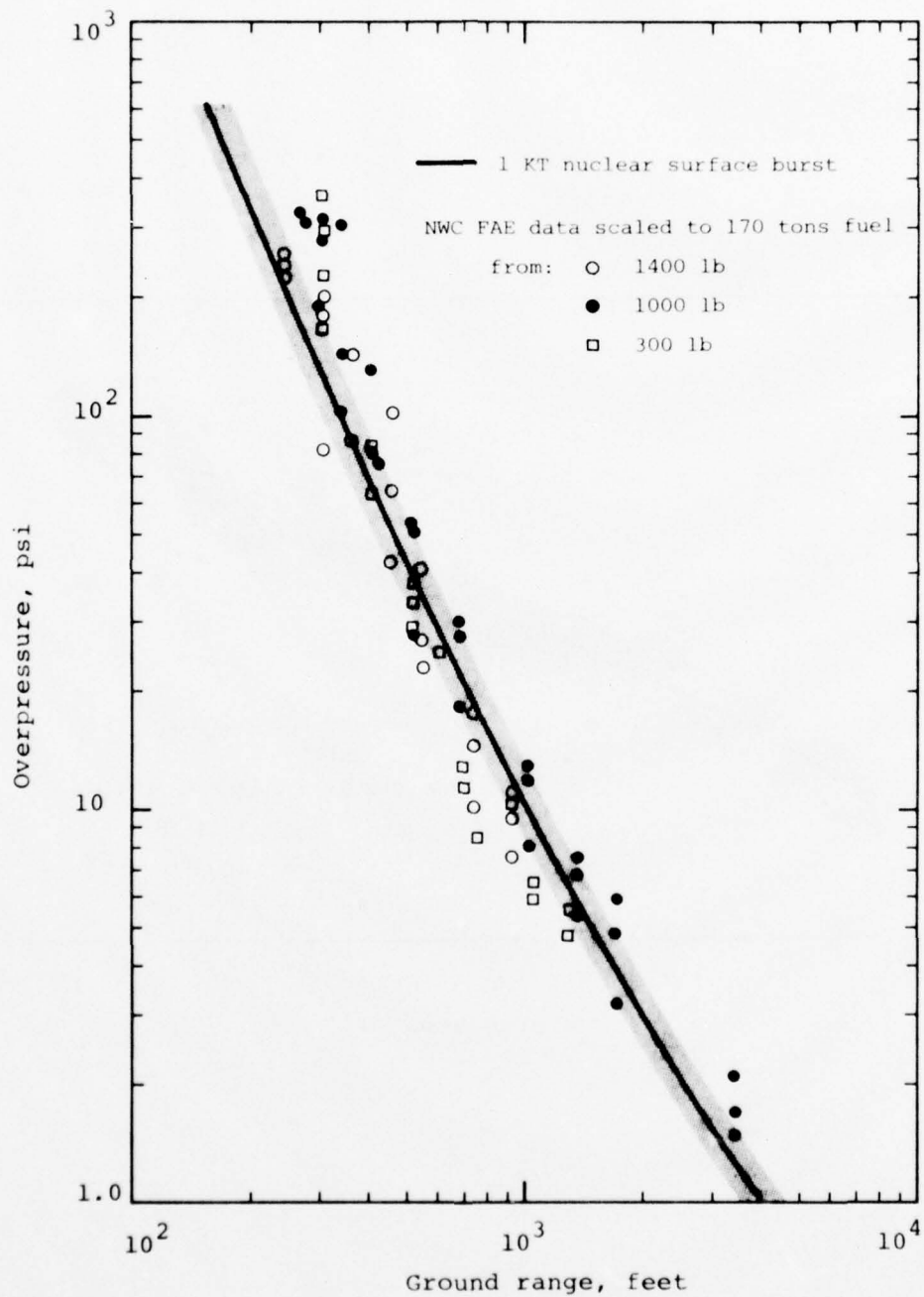


Figure 6 Scaled overpressure for ethylene oxide FAE compared with overpressure from a 1-KT nuclear surface burst. (Shaded areas show scatter of nuclear data.)

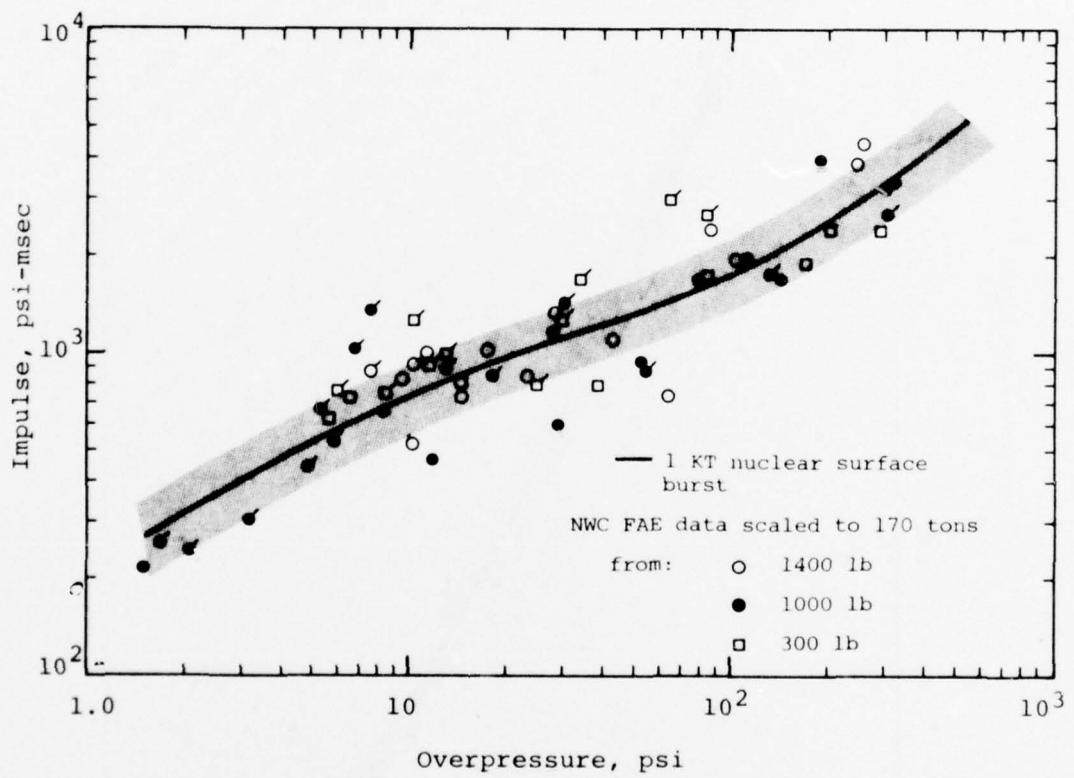


Figure 7 Scaled overpressure impulse for ethylene oxide FAE compared with impulse from a 1-KT nuclear surface burst. (Shaded areas show scatter of nuclear data.)

The data (Figures 6 and 7) indicated that 170 tons of ethylene oxide, explosively disseminated and detonated in a cloud geometry geometrically similar to the smaller detonations, would be required to simulate a 1-KT nuclear surface burst. Thus, it appears this FAE configuration is somewhat more than twice as efficient (on a fuel-weight basis) as condensed explosives.

Reference 11 gives data on the detonation of six BLU-73/B warheads containing 72 pounds of ethylene oxide. Airblast measurements were made along three lines located at 0, 120, and 240 degrees azimuth. Detonators were placed along the zero degree direction for two explosions, along the 45 degree direction for two explosions, and along the 180 degree direction for the remaining two explosions. Meteorological conditions ranged over temperatures from 70- to 98-°F with winds varying from 5- to 35-mph.

Overpressure impulse data are plotted as a function of overpressure in Figure 8. Since the reference presents no waveforms, it was not possible to run a check on maximum overpressures as was done for the NWC data. The overpressure data along the gage line located at 240 degrees was consistently higher than the overpressure data along the line at zero degrees azimuth and it appeared that the placement of the detonators had a clear effect on maximum overpressure. The variation in overpressure impulse was less pronounced than for overpressure and the data along the gage line at 240 degrees was only slightly higher than the data along the line at zero degrees without any clear effect of detonator placement.

The fuel cloud appeared to have two families per cloud volumes, $1.14 (\pm 0.02) \times 10^4 \text{ ft}^3$ and $1.43 (\pm 0.09) \times 10^4 \text{ ft}^3$.

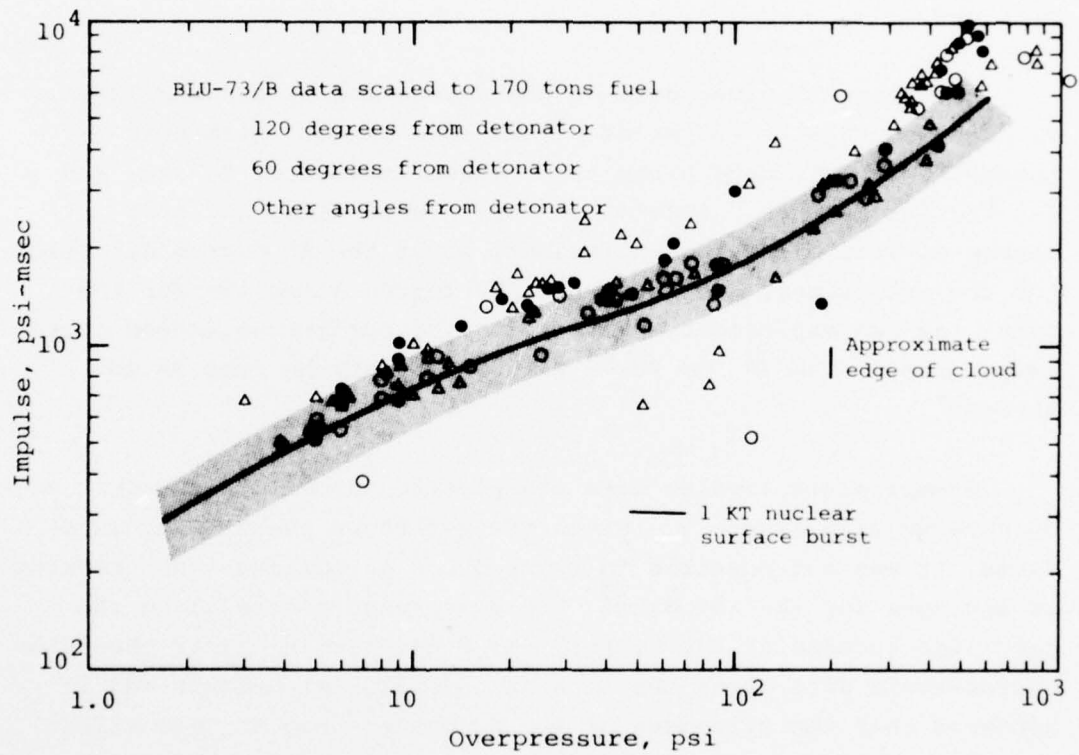


Figure 8 Scaled overpressure impulse for BLU-73/B warheads compared with impulse from a 1-KT nuclear surface burst. (Shaded area shows scatter of nuclear data.)

These cloud volumes imply fuel concentrations of 8.5 percent and 6.8 percent, respectively. Data also indicate two families of detonation velocity, 6,088 (± 379) ft/sec and 4,750 (± 373) ft/sec, but since the cloud volumes (and consequent fuel concentrations) were reported independent of the detonation velocity measurements it was not possible to correlate the two sets of data.

Two observations can be made from the data plotted in Figure 8. First the data, except for a few wild points, do not scatter appreciably more than the data from the larger charges shown in Figure 7; second, the smaller charges appear to be more efficient, i.e., they have a larger impulse when scaled to 170 tons of fuel than do the data from the larger charges. It should be noted that for the 300 to 1400 pound charge data, there is a small but consistent tendency for the impulse efficiency to decrease with increasing fuel weight which is consistent with the difference noted between the data of Figures 7 and 8. This result is probably the effect of depletion of fuel droplets by the ground surface due to insufficient height-of-burst of the fuel canister (Reference 12). However, a study (Reference 13) of the effect of height-of-burst on the output of standard BLU-73/B canisters indicated no significant differences appearing in the airblast for heights-of-burst ranging from 3 to 18 feet. This lack of airblast degradation was attributed to the change in cloud shape at larger heights-of-burst which allowed the cloud thickness to increase, thus maintaining approximately constant shock relief distance over the range of cloud formation heights.

3.3 HEMISPHERICAL BALLOONS FILLED WITH FUEL-AIR MIXTURES

Reference 14 reports airblast data from detonations of hemispherical balloons inflated by near stoichiometric mixtures of MAPP* and air. The hemispheres were centrally detonated at

* A mixture of methylacetylene, propadiene, and propane fuel used as a welding gas.

ground level and airblast measured along two radial lines 120° apart. Five-, 10-, and 20-meter diameter hemispherical balloons were used with nominal fuel weights of 6.5-, 52-, and 40-pounds, respectively.

Although fuel was sprayed into the balloons over a large area, failure to achieve FAE detonations on early tests led to the suspicion that seepage into the ground inhibited vaporization of the liquid resulting in fuel-to-air ratios outside of the detonability limits. On subsequent tests, black polyethylene plastic was laid over the ground inside the enclosure to preclude cloud depletion. To achieve a homogeneous mixture, fans were used inside the inflated hemispheres to circulate the MAPP gas and air. One, four, and eight fans were used in the 5-, 10-, and 20-meter diameter hemispheres, respectively. Mixing time varied from approximately 20 minutes for the 5-meter diameter hemisphere to 170 minutes for the 20-meter diameter hemisphere.*

Data in the report are not tabulated so it is not possible to distinguish between individual data points along the two blast lines or between sets of data for the different hemisphere diameters. Consequently the data had to be analyzed on the basis of the maximum spread in impulse associated with the maximum spread in pressure reported at a particular range. These data, corrected to STP, were scaled to a common denominator of 1 pound of MAPP for both the overpressure-distance curve and the overpressure impulse-overpressure curve. When fitted to the 1-KT

* It should be noted that up to 2 hours and 15 minutes were required to inflate the 20-meter diameter hemispheres and that winds severely stressed the partially inflated hemispheres and sometimes caused tears at the anchor boundary. Experience showed that inflation could not be attempted in winds greater than 10 mph. Once inflated the hemispheres were stable and withstood gusts up to 15 mph.

nuclear surface burst curves, the overpressure-distance relationship (Figure 9) shows a different fuel efficiency than does the overpressure impulse-overpressure curve (Figure 10). In either case, the FAE fuel efficiency is greater than that for the explosively disseminated canister of ethylene oxide.

This is believed due to the more controlled nature (particularly the controlled mixing of fuel and air) of the hemispherical balloon detonations and to the more efficient cloud geometry (hemispherical versus cylindrical) to be discussed in the next section. The fact that it takes only 63 tons of fuel to match the impulse-overpressure curve whereas it takes 88 tons of fuel to match the overpressure-distance curve is also believed to be a function of the cloud geometry. An interesting comparison point to the MAPP-air hemisphere data is the propane-oxygen hemisphere data on Reference 1 (Figure 11), where 88 tons of fuel (propane) are required to fit the impulse-overpressure curve for the 1-KT nuclear surface burst.

3.4 SUMMARY

Figures 1, 6, and 9 and Figures 2, 7, 10, and 11 show that for both the condensed explosives and FAE there are occasional points which fall low in both overpressure or overpressure impulse with respect to the general trend of data. However, the FAE data, in general, exhibit a wider variability than do the data from the high-explosive nuclear-airblast simulation experiments. In quantitative terms, the high-explosive impulse data have a standard deviation about the mean ($\pm\sigma$) of approximately ± 10 percent, while the standard deviation for both sets of hemispherical balloon data is approximately ± 20 percent and the standard deviation for FAE impulse data is approximately ± 30 percent. Thus it appears that FAE, even those under the most controlled conditions, do not approach the prediction accuracy for condensed explosives.

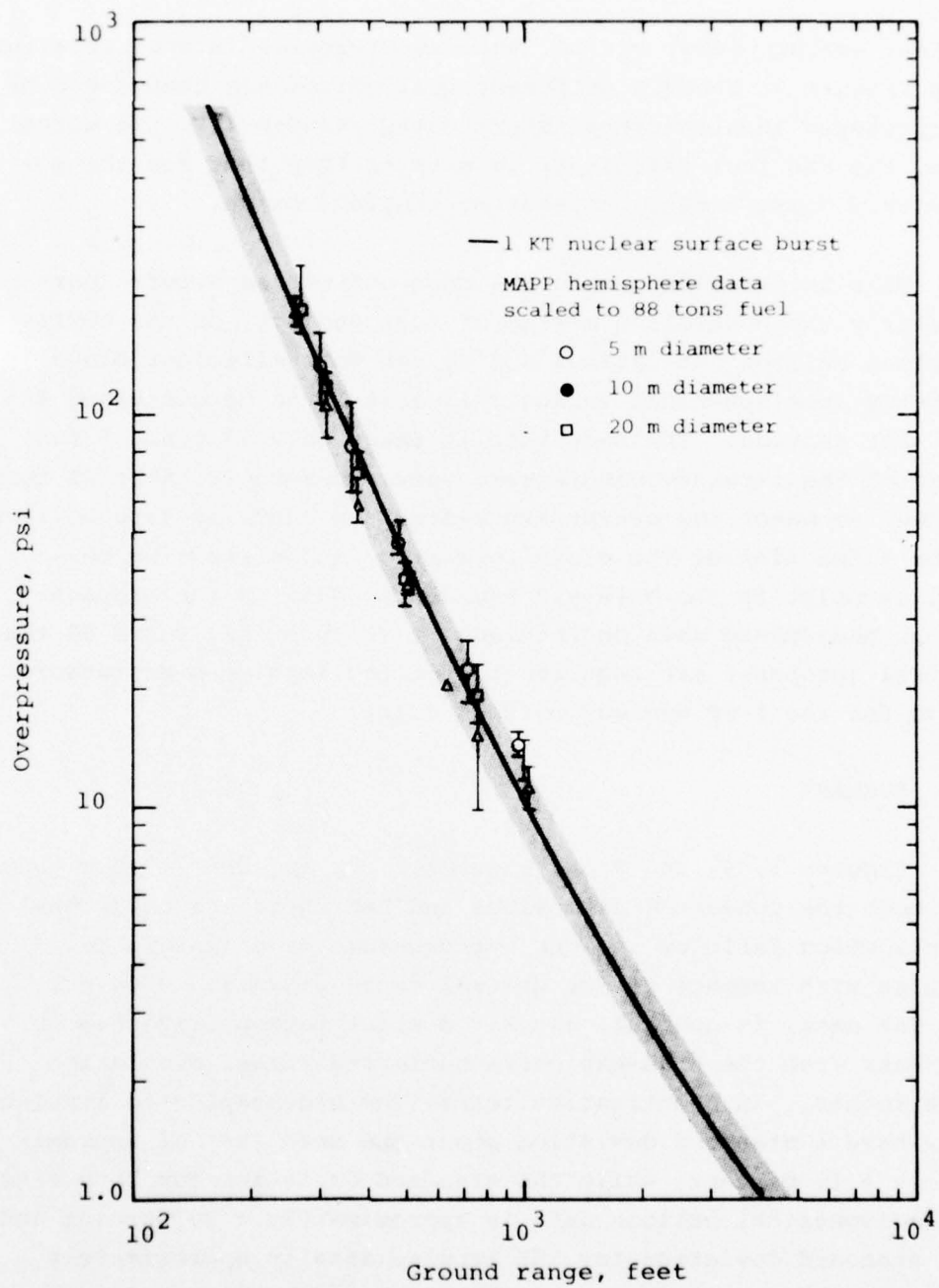


Figure 9 Scaled overpressures for MAPP-air explosions compared with overpressure from a 1-KT nuclear surface burst. (Shaded area shows scatter of nuclear data.)

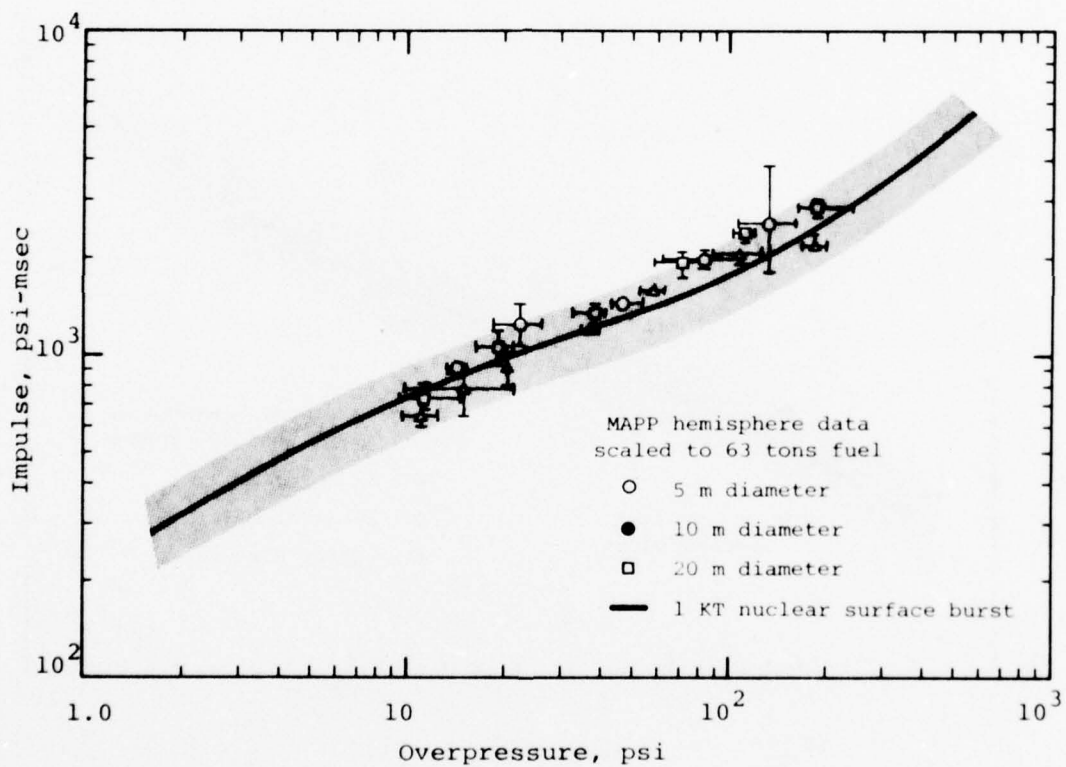


Figure 10 Scaled overpressure-impulse for MAPP-air explosions compared with impulse from 1-KT nuclear surface burst. (Shaded area shows scatter of nuclear data.)

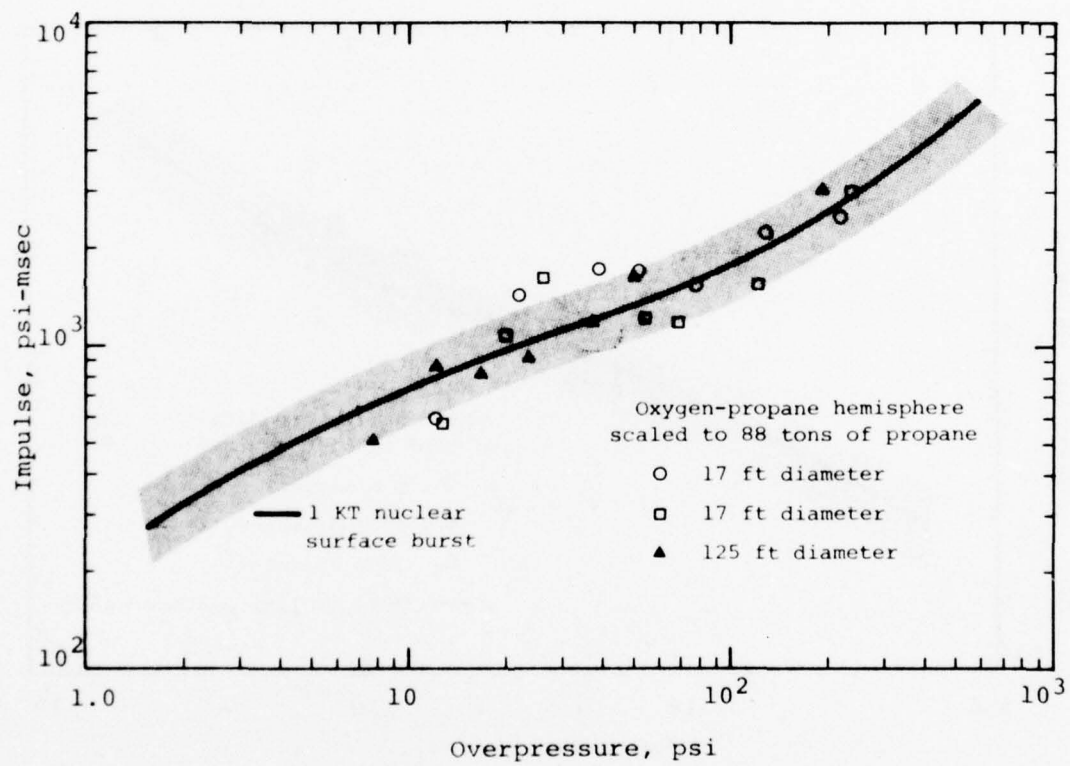


Figure 11 Scaled overpressure-impulse for propane-oxygen explosions compared with impulse from 1 KT nuclear surface burst. (Shaded area shows scatter of nuclear data.)

The data do not support the hypothesis put forth in Reference 3 that larger FAE would result in smaller error bands. Some of the data scatter for the smaller FAE events, i.e., the data from the BLU-73/B, may be due to instrumentation. However, the larger data scatter of Figure 8 over that of Figure 7 appears to be associated with the data scatter in different measurement directions rather than from differences between data on different events. The scatter in data along different directions on the same event is to a large extent associated with the off-center detonation of the cloud influencing the airblast and illustrates the necessity, for nuclear-airblast simulation purposes, of providing a uniform fuel distribution within the cloud and centrally detonating the cloud.

The nuclear equivalency of FAE varies from an upper limit of 170 tons of fuel per kiloton for explosively disseminated clouds to a lower limit of 63 tons of fuel per kiloton for well mixed, centrally detonated fuel-air mixtures contained in hemispherical balloons. This lower limit appears too low when compared with data from propane-oxygen detonations. For well distributed, unconfined aerosol clouds of cylindrical shape, having a height-to-diameter ratio of ~ 0.2 , the nuclear equivalency is expected to be approximately 150 tons of fuel per kiloton, somewhat smaller than for the explosively disseminated clouds but substantially larger than for premixed, hemispherically shaped fuel vapor-air mixtures.

SECTION 4

EFFECT OF CLOUD GEOMETRY AND WIND ON SIMULATION EXPERIMENT DESIGN

Calculations of the airblast from ideal detonations of cylindrically shaped ethylene oxide clouds have been carried out in Reference 15. An overpressure impulse-overpressure curve for several cylinder diameter-to-height ratios may be constructed from these results (Figure 12). This presentation shows that as the diameter-to-height ratio of the cylinder increases, the nuclear efficiency of the cloud decreases. The explosively disseminated fuel clouds have a diameter-to-height ratio of approximately five (height-to-diameter ratio equals 0.2) and have an average fuel concentration of approximately 8 percent. For 170 tons of fuel, the clouds have a height of 140 feet and a diameter of 700 feet. Figure 12 indicates that by going to a diameter-to-height ratio of unity it may be possible to achieve a factor of 2 greater fuel efficiency and hence a reduction in cloud volume by a factor of 2. Assuming this one arrives at a cloud height and diameter of 325 feet. Going to a diameter-to-height ratio of 10 would decrease the fuel efficiency to half that for the diameter-to-height ratio of 5 and consequently double the volume requirements of the cloud. This cloud would be 110 feet in height and 1110 feet in diameter.

The highest fuel efficiency represented in the data was 63 tons of MAPP (this would result in a diminished overpressure-distance curve which could be accounted for by placing the

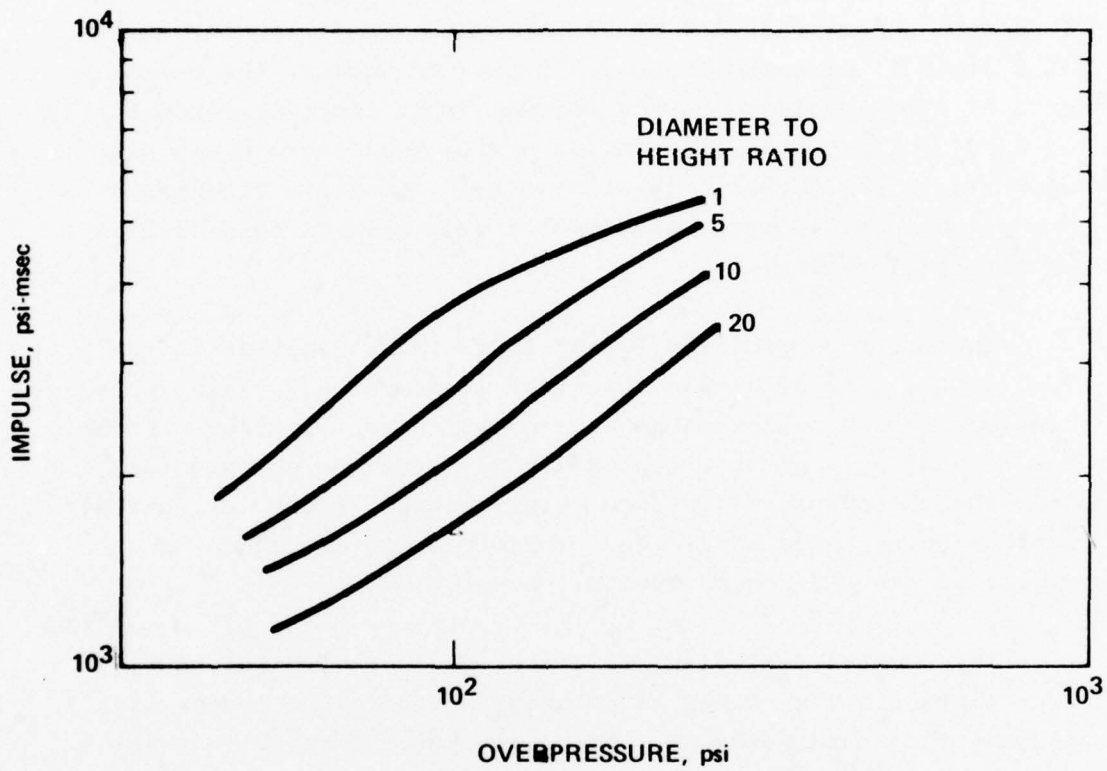


Figure 12 Calculated overpressure impulse as a function of overpressure scaled to source energy of 10^{12} cal (1-KT).

target points closer to ground zero as previously discussed) and a resulting hemispherical cloud (again at a fuel concentration of 8 percent) of approximately 210 feet in radius, the height of a 21 story building. Even for the upper limit of detonability of MAPP of 13 percent, the radius of the hemisphere would be approximately 175 feet. These numerical exercises illustrate the gigantic scale over which fuel clouds must be more-or-less uniformly disseminated.

The other controlling factor in the dissemination of the fuel is the time available such that wind does not cause appreciable error in overpressure at a given target location. Error due to wind at a given overpressure level can be calculated assuming the pressure-distance relationship for the 1-KT nuclear surface burst to be simulated. These results are shown in Figure 13 for a 3-second fuel dispersal time.

For a given fuel dispersal time, a given wind velocity represents a given change in location of the cloud center with respect to ground zero, ΔR . Since the percent error in overpressure is proportional to $\Delta R/R$, the largest errors in overpressure occur at the larger overpressures. Although the assumption of a 3-second dispersal time is somewhat arbitrary, Figure 13 shows that dispersal times of this order are necessary to keep overpressure errors realistically less than 20 or 30 percent. Since the errors are proportional to the wind velocity times dispersal time, if velocities as low as 2 knots could be assured, then dispersal times could be as long as 10 to 15 seconds for the same errors shown in Figure 13. To design a system dependent upon such low wind velocity at shot time seems, however, impractical at this stage because of the low probability of occurrence of such low wind velocities on any given shot day and the generally large costs associated with shot delays.

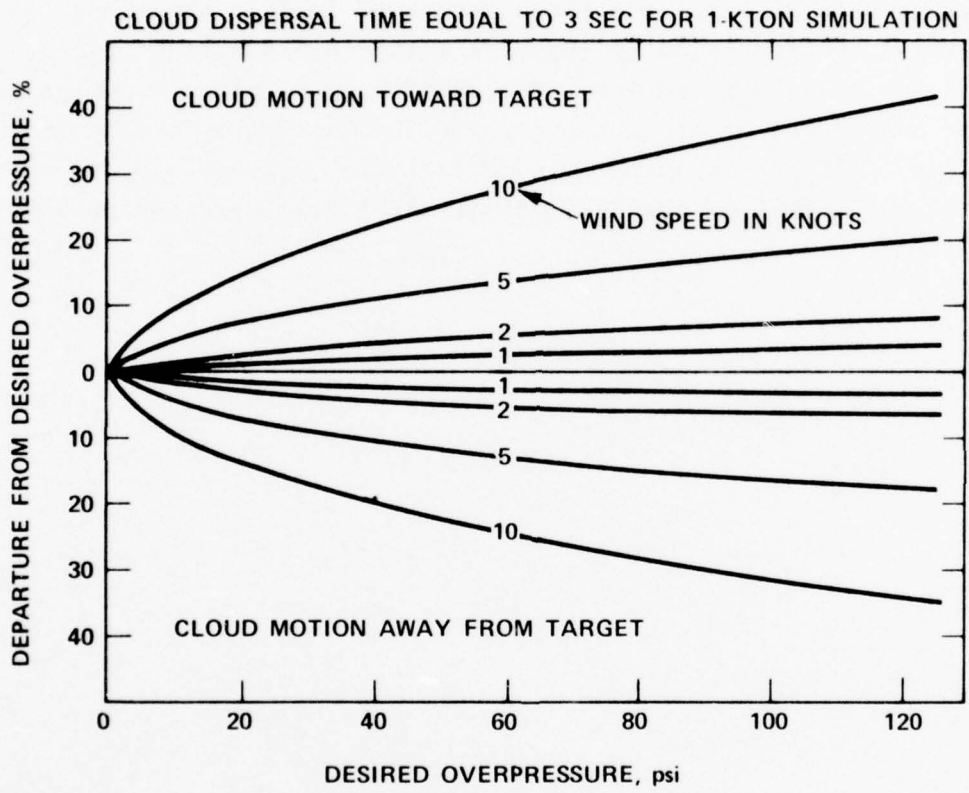


Figure 13 Error in predicted overpressure due to cloud translation by wind.

Fuel rates, cloud volumes, and fuel-dispersal time limitations discussed above tend to bound the system requirements. Obviously to disperse the large amount of fuel in the times dictated by wind velocity requires multiple dispersion points. Just how this is to be done, the efficiency to which vaporization and mixing of air and fuel, and the uniformity and control of the fuel concentration in such gigantic volumes is believed to be the kernel of the FAE nuclear-airblast simulation problem.

SECTION 5

DETONABILITY OF AEROSOL-AIR MIXTURES

Two academic institutions: The University of Michigan (UM) under the direction of J. A. Nichols and the University of California at Berkeley (UCB) under the direction of A. K. Oppenheim have done extensive research into the combustion and detonation of fuel-oxidizer mixtures. The work at UCB has been heavily weighted toward theoretical investigation while the UM group has concentrated on the experimental aspects of detonability. Experimentally it has been found that the detonability of a fuel-air mixture is controlled by two factors; the mean droplet size and the average fuel concentration. Both of these factors can be varied over quite wide ranges and the mixtures will still support a detonation.

Results from the UM group indicate that a mixture of air and a fuel composed of uniform size droplets less than 2500 microns in diameter can support a detonation. If the liquid component of the mixture is composed of droplets having diameters of less than ten microns, the resulting mixture will have detonation properties close to the theoretical Chapman-Jouquet (CJ) conditions as computed from the gaseous mixture* (Reference 16). As the droplet size increases from 10 microns, a time lag between passage of the shock front and conflagration of the droplet is developed. This delay consists primarily of the time required

* Reference 16 indicates that the ideal CJ shock velocity may be exceeded for one-dimensional detonations in fogs with mean droplet diameters of around 2 microns.

for the passing shock front to shatter the droplet. As the time delay increases, shock velocities lower than the ideal CJ values are observed (Reference 17).

The amount of energy as a function of fuel concentration required to initiate the detonation was found to be a minimum near the stoichiometric value, with a factor of 1.5 about the stoichiometric being the practical limits on the concentration that can be detonated (Reference 18). This effect can be seen in Figure 14.

It has also been shown (Reference 19) that combustion of the droplet can be initiated by the passage of the shock front alone. Furthermore, the energy released during the conflagration of the droplets augments the energy in the shock front. In diverging geometry, with the absence of any energy augmentation, a shock front will die out. The peak pressure of the shock front can only be maintained if a certain minimum amount of energy is added to the shock front as it diverges. Consequently there is a minimum fuel concentration which can maintain a shock front in diverging geometry (References 20 and 21).

Experiments using mono-disperse sprays of kerosene, with droplet sizes between 200 and 600 microns, are reported in Reference 21. To investigate the characteristics of a detonation in a divergent geometry, a cylindrical apparatus was used. Data from these experiments are seen in Figure 15. A similar study was performed using diethylcyclohexane (Reference 17) and a much larger range of drop diameters. Results of this work are shown in Figure 16. The tests reported in Reference 17 were conducted over a concentration range between 20 percent and 100 percent of stoichiometric. Reference 17 attributes the

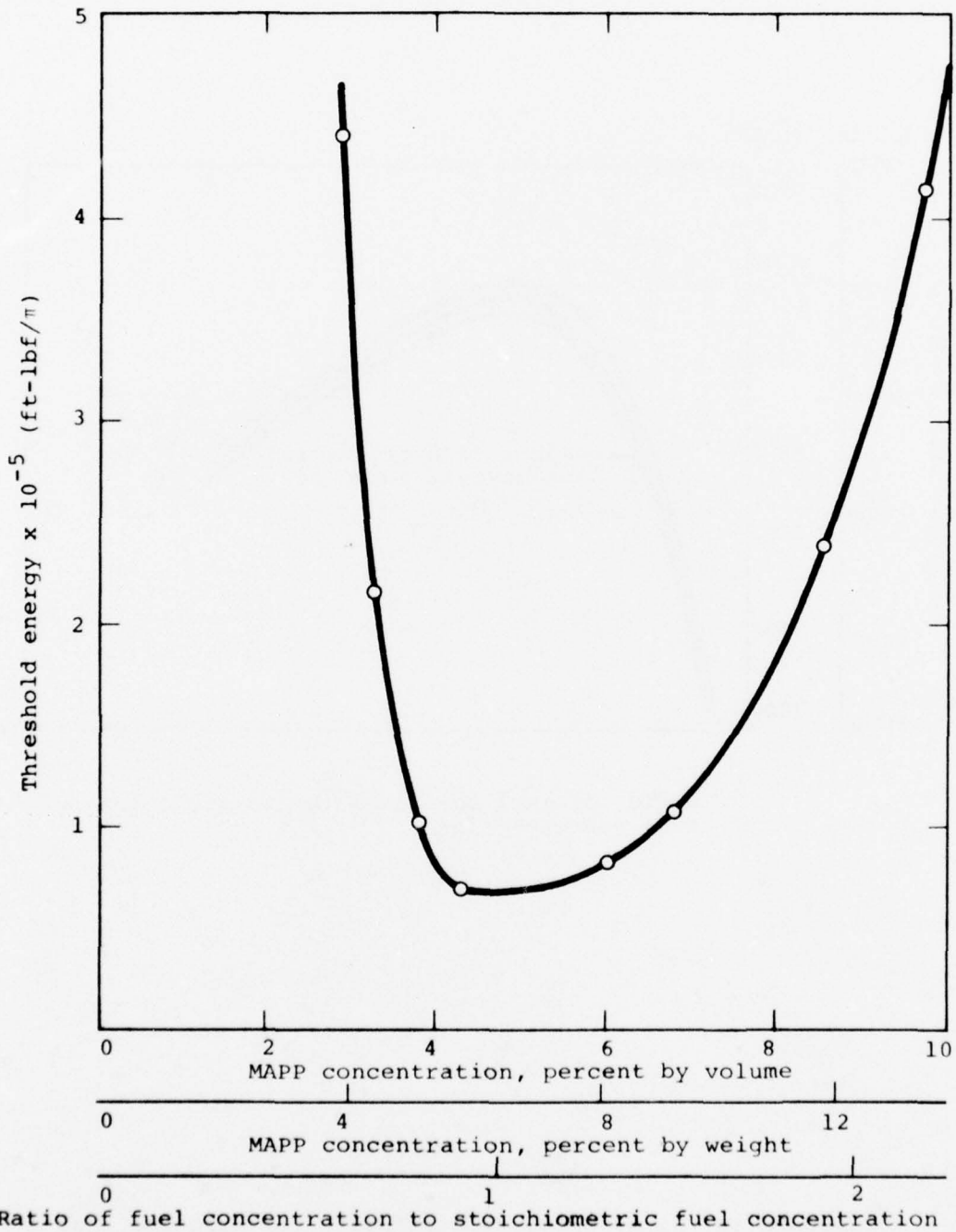


Figure 14 Critical threshold energy for detonation initiation as a function of MAPP concentration in air (from Reference 18).

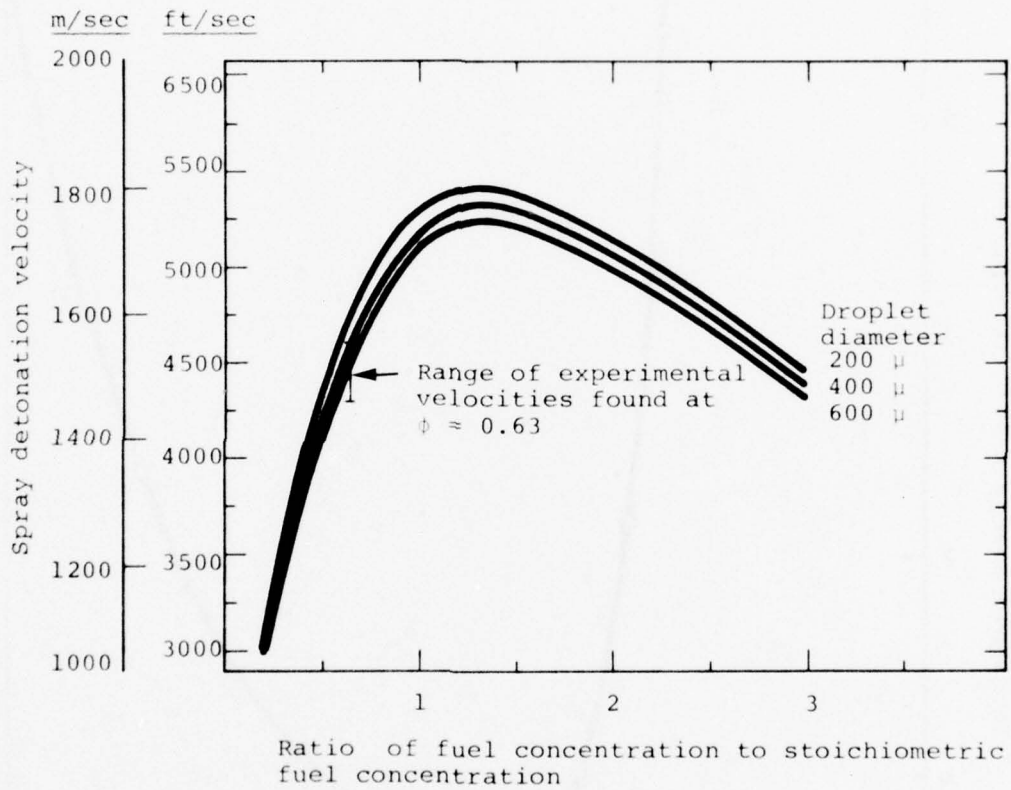


Figure 15 Spray detonation velocity for Kerosene 2 as a function of equivalence ratio and drop size (from Reference 21). (Solid lines are theoretical estimates.)

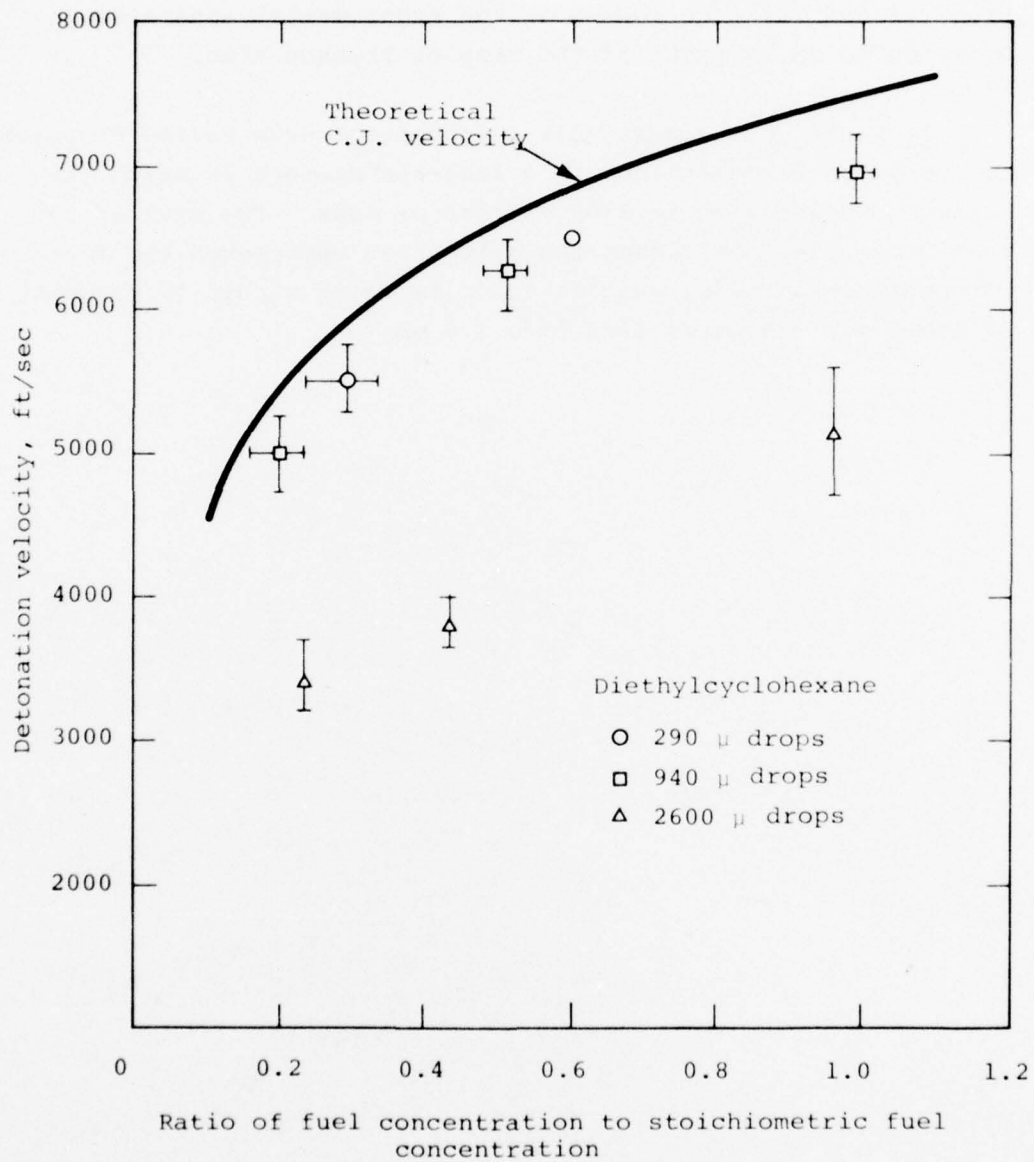


Figure 16 Comparison of experimental detonation velocity with the ideal CJ velocity (from Reference 17).

degradation in performance with increasing drop size to heat transfer and friction losses in the experimental apparatus in addition to an increase of the droplet breakup time.

It would thus appear that a detonation wave having diverging geometry can be maintained in a fuel-air mixture in which the maximum droplet size is 2500 microns or less. The smaller the mean drop size, the closer the detonation approaches the ideal CJ conditions, the detonation velocity being within 10 percent of ideal for diameters less than 1.0 mm.

SECTION 6

SPRAY NOZZLE TECHNOLOGY REVIEW

6.1 NOZZLE PERFORMANCE

References 3 and 5 concentrate on nozzles as a means for fuel dispersal without giving sufficient backup on available nozzle performance to establish feasibility of the method. To establish a data base, numerous U.S. manufacturers were contacted. The data on nozzle performance thus obtained are shown in Table 1. The ease of extracting information appears to be a strong function of the company size. Those manufacturers with a large and varied product line were found to be extremely helpful, while the smaller companies with a limited and proprietary line were quite reluctant to disclose details of their products.

A rough estimate of the nozzle performance required can be obtained by referring to Section 3.4: approximately 150 tons (50,000 gallons) of fuel in a cloud approximately 140 feet high and 720 feet in diameter. Further, this cloud is to be generated in approximately 3 seconds. This dictates a total flow of approximately 10^6 gallons per minute. If 300 nozzles are used in the simulation system, each nozzle would have to pass about 3300 gallons per minute. Several manufacturers list nozzles within this flow rate capability (Table 1). More difficult to obtain is the required vertical reach of approximately 140 feet. Several manufacturers document a horizontal reach, given an initial flow vector, however, documented data on vertical reach are nonexistent. The vertical reach values of Table 1 were obtained verbally.

TABLE 1 SURVEY OF U.S. NOZZLE MANUFACTURERS

MANUFACTURER	STATE	DROP SIZE	FLOW RATE (gpm) AT (psi)	SPRAY ANGLE (deg)	REACH (ft)	TYPE OF PRODUCT (PRIMARY)
BETE FOG	MASS	YES	945 100	120	ND	FOGGING NOZZLES
SPRAYING SYSTEMS CO.	ILL	YES	21→4500 100	~100	ND	ALL FORMS (POSSIBLY LARGEST IN U.S.)
SPRAY ENGINEERING	MASS	YES	4100 60	80→90	ND	AGRICULTURE AND COOLING
WESTERN FIRE EQUIPMENT	CAL	NO	500 100	10	90	FIRE EQUIPMENT
STANG MFG. CO.	CAL	NO	5000 200	ND	100	LARGE SCALE REMOTE FIRE EQUIPMENT
MONARCH MFG. WORKS	PA	NO	1430 100	80	ND	FUEL (OIL BURNER) EQUIPMENT
ECODYNE CORP.	CAL	CLAIM NOZZLE DESIGN AND PERFORMANCE ARE PROPRIETARY—NO DATA DISCLOSED				COOLING TOWERS
SANTA ROSA MFG.	CAL	NO DATA OVER PHONE, NO CATALOGS				FIRE EQUIPMENT
LA FAVORITE	NJ	NO DATA OVER PHONE, NO CATALOGS			< 100	FIRE EQUIPMENT
DELAVAN	IA	YES	78 500	70	ND	FUEL (OIL BURNER) EQUIPMENT
AGROTECH INC.	Md	OUTLET OF SPRAYING SYSTEMS COMPANY				
SIERRA FIRE EQUIP. (ELKART BRASS)	CA (Ind)	CLAIMED NOT TO HAVE EQUIPMENT APPLICABLE TO OUR PURPOSES				

Water atomization performance of the nozzles from two different manufacturing companies are displayed in Figures 17 and 18. The flow rate performance of the nozzle from the Spraying Systems Company are as follows: Model No. H20 is one of a long line of full-cone, large capacity nozzles. The largest orifice diameter for the H20 in this series is 9/16ths of an inch and, at 100 psi head pressure, has a flow rate of 68 gallons per minute. Nozzle type G1 is a much smaller device, having a flow rate of 0.3 gallons per minute at a head pressure of 100 psi. What is significant about Figure 17 is that if the data may be extrapolated to very high pressures, even the highest flow rate nozzles may produce particle droplets on the order of 1000 microns in diameter. The nozzles from the Bete Fog Nozzle Company (Reference 22, represented in Figure 18), are self-explanatory. Here again, if the data can be extrapolated to 1000 gallons per minute at 1000 psi head, droplet sizes will still remain less than 1000 microns.

For obvious reasons, it is highly desirable to be able to performance-test candidate nozzles using water as the working fluid. To be able to use these data, it is necessary that performance-correlation rules between water and the candidate hydrocarbon fuels exist. Because of the internal design of many commercial nozzles, this is not always possible (Reference 23). However, some approximate guide lines have been developed.

Droplet size and nozzle flow rates are governed, in addition to pressure head, by the material properties viscosity, surface tension, and liquid density. Under ideal conditions, the flow rate through a nozzle is given by

$$\Omega = \frac{k}{\eta} \sqrt{\frac{\Delta P}{\rho}} \quad (1)$$

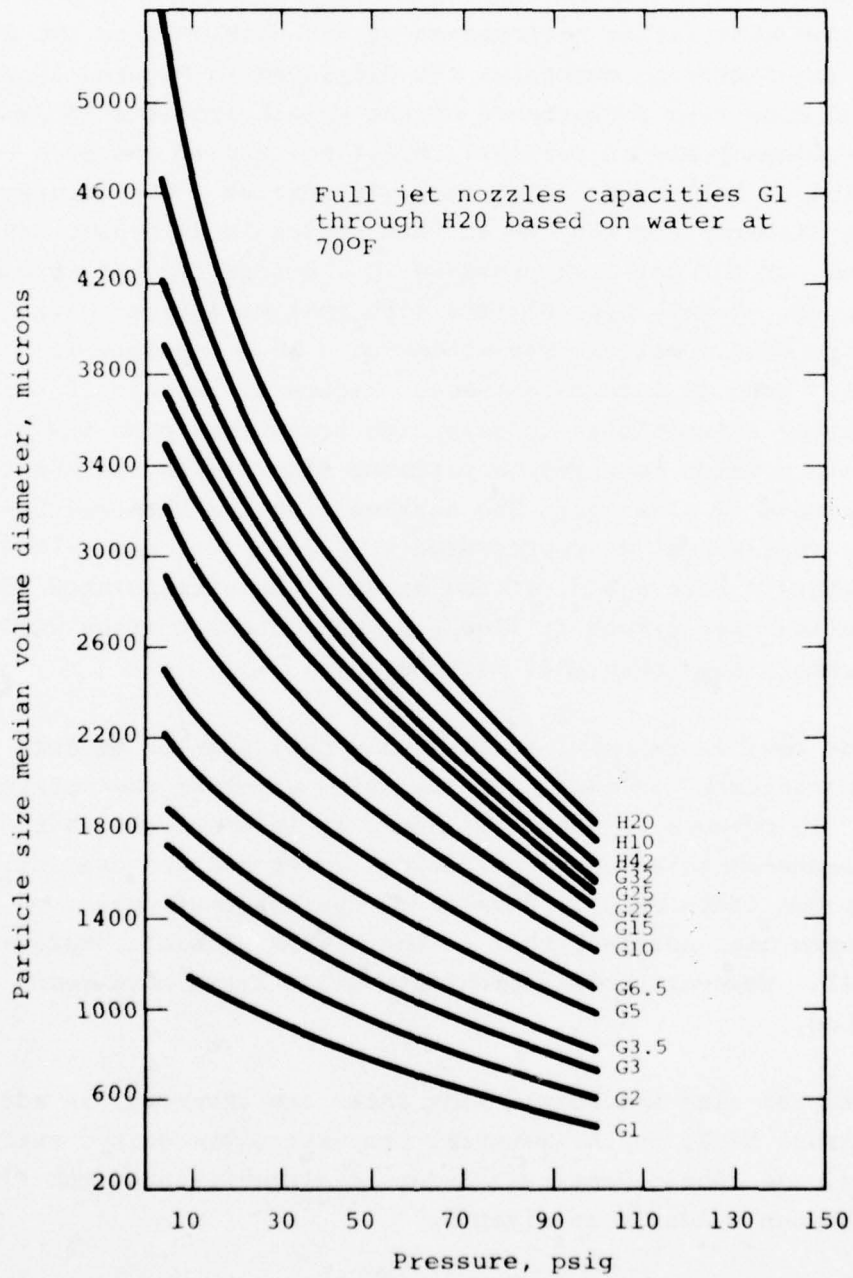


Figure 17 Spray particle size versus pressure (from Spraying Systems Company Dwg. No. 11825, Reference 23).

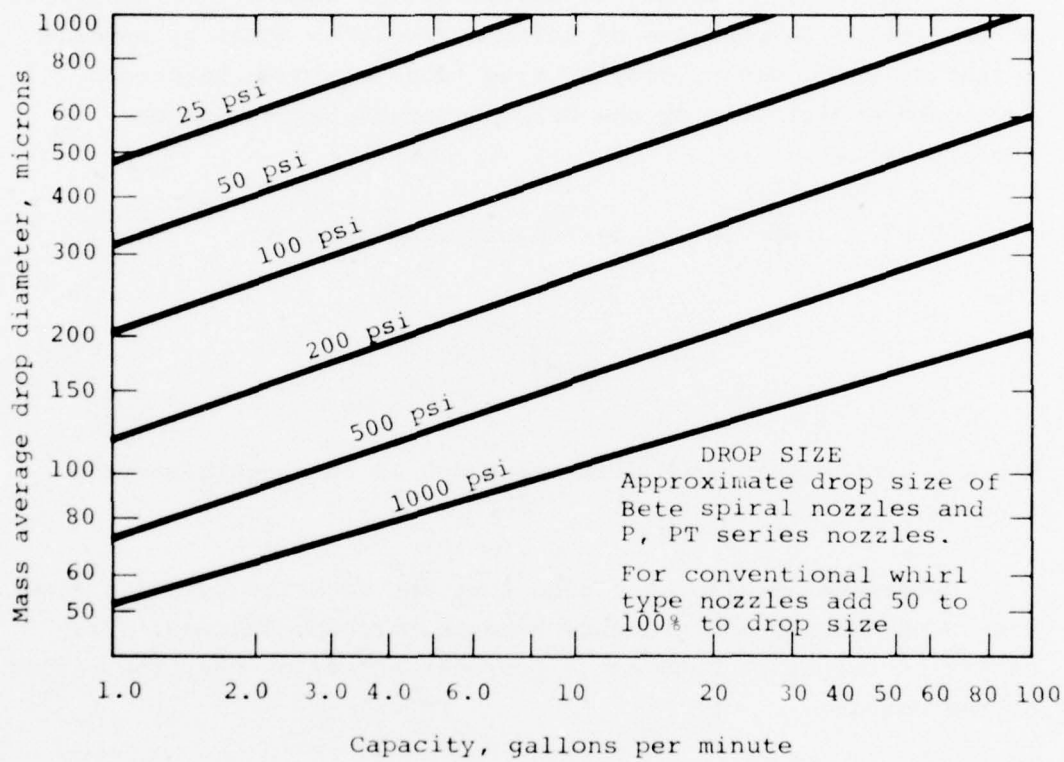


Figure 18 Mean drop diameter versus flow rate and pressure drop across nozzle (from Reference 24).

where k is a constant, Δp is the pressure head, ρ is the liquid density, and η is the dynamic viscosity.

In those cases where the nozzle design admits the possibility of predicting performance of using hydrocarbon fuels by experimentation using water, droplet size rules-of-thumb have been developed empirically by the Delevan Manufacturing Company (Reference 24).

Droplet diameter may be roughly estimated by

$$\bar{d} \sim \left(\frac{\eta}{\Delta p} \right)^{1/3} (\sigma)^{1/4} \quad (2)$$

where \bar{d} is the mean drop diameter and σ is the liquid surface tension.

Reference 24 also concludes that the equation relating flow rate with density and pressure head is only approximate. Viscosity on the other hand has a profound effect on the flow rating of the nozzle:

"The effect of viscosity is complex, under certain conditions a higher viscosity will increase flow rate. Sometimes it has the opposite effect. In cone spray nozzles, a moderate increase in viscosity is likely to increase flow. At higher viscosities and with other types of nozzles the flow rate usually decreases with an increase in viscosity. The exact effect must be determined experimentally for the specific nozzle design and operating conditions involved."

Thus, the use of water in a particular nozzle for its calibration must be done with caution.

Surface tension is a slowly varying function of temperature and, for hydrocarbon fuels, is approximately one-third that of water. The viscosity is a very strong function of temperature. However, for most of the fuels under consideration, it is approximately one-third that of water at normal room temperature.

The use of water to simulate the hydrocarbon fuel should not be ruled out automatically. The viscosity of water can be reduced by a factor of three by raising its temperature to 45°C (Reference 25) and the surface tension may be reduced by addition of wetting agents. It is thus conceivable that the viscosity and surface tension of candidate hydrocarbon fuels can be approximated by the use of water under specific temperature and additive conditions. The only property that cannot be matched is density.

In any case, not even water performance data exist at the high pressure and flow rate conditions required for a 1-KT simulation. A basic experimental program would be required to obtain such information.

6.2 THEORETICAL VERTICAL REACH

From Section 5, it is clear that droplets having mean diameters of less than 2500 microns are required to maintain a detonation front. Assuming Stokes law, the equation of motion of a droplet travelling through the air is given by

$$\frac{dv}{dt} = -g \left(\frac{v}{v_t} + 1 \right) \quad (3)$$

where g is the gravitational acceleration and v_t is the terminal free-fall velocity of the droplet in air.

It is pointed out in Reference 26 that only droplets having diameters less than 80 microns will obey Stokes law. For diameters between 80 and 8000 microns it is claimed that liquid droplets falling in gases appear to remain spherical and deviate from Stokes law in the same manner as solid spherical particles, up to a Reynolds number of about 500.

Solution of Eq. (3) leads to the following equation for the maximum height of the particle when initially projected vertically upward.

$$h_{\max} = \frac{v_t}{g} \left[v_0 - v_t \ln \frac{(v_0 + v_t)}{v_t} \right] \quad (4)$$

where v_0 is the initial upward velocity of the droplet.

As an example of what might be expected from a commercially available nozzle, consider Spraying Systems Company nozzle 8HF800 (Reference 27). This device has an orifice diameter of 4.031 inches and can deliver 2800 gallons per minute at a pressure of 100 psi. The mean flow velocity through this orifice is then 72.6 ft/sec. This is a spray nozzle having a wide-angle dispersion pattern; however, for the sake of argument, let us assume that all flow is vertically upward. Using terminal velocity data given in Reference 26, Table 2 has been created. Most nozzle manufacturers indicate the flow rate through their nozzles is proportional to the square root of the pressure head. Thus for the nozzle considered above, if the pressure were increased to 1000 psi, it would perform at 8850 gallons per minute and would have an accompanying 230 ft/sec flow velocity. Data corresponding to this initial velocity are also listed in Table 2.

TABLE 2 MAXIMUM DROPLET ALTITUDE AS A FUNCTION OF DIAMETER AND INITIAL VELOCITY (v_o)

Drop Diameter (μ)	Terminal Velocity, v_t (ft/sec)	Maximum Height, (ft)	
		$v_o=72.6$ ft/sec	$v_o=230$ ft/sec
2600	24.8	29.8	133
1500	18.5	24.8	105
1000	13.2	19.6	78.5
500	6.8	11.8	43.5
100	0.91	1.9	6.4

Terminal velocities different from those quoted in Table 2 may be obtained from Reference 27 (Table 3). If these latter data are used instead of those from Reference 22, the maximum height for a 1500 micron diameter droplet at a pressure head of 1000 psi is approximately 61 feet (compared with 105 feet, Table 2).

These are maximum estimates of the particle trajectory height. If the actual drag coefficients were used, the higher-order velocity dependence would have resulted in a greater drag upon the particle and a lower trajectory. Furthermore, droplet ablation will occur due to both evaporation and shattering. It is unlikely that a 2500 micron diameter particle existing near the nozzle throat will have the same size at its zenith. This also contributes to a lower maximum height for the droplet.

In the absence of effects other than those considered above, it is improbable that single droplets can be projected to the heights requisite for the feasibility of a 1-KT simulation.

TABLE 3 WATER DROPLET COMPARISON DATA
(FROM REFERENCE 27)

<u>Particle Size Range (μ) Median Volume</u>	<u>Comparative Subject in Particle Size</u>	<u>Time for Particle to Fall 10 Feet (sec)</u>	<u>Drift in 3 mph Wind 10 Feet Fall (ft)</u>
5000 to 2000	Heavy Rain	0.85	3.5
		0.9	4.0
2000 to 1000	Intense Rain	0.9	4.0
		1.1	5.0
1000 to 500	Moderate Rain	1.1	5.0
		1.6	7.0
500 to 100	Light Rain	1.6	7.0
		11.0	48.0
100 to 50	Misty Rain	11.0	48.0
		40.0	175.0
50 to 10	Wet Fog	40.0	175.0
		1020.0	4500.0
10 to 2.0	Dry Fog	25400.0	112000.0
1.0 to 0.1	Fumes	Suspended	in air --
0.01 to 0.001	Smoke	Suspended	in air --
Below 0.001	Molecular Dimensions	--	--

6.3 SUMMARY

We have been unable to uncover experimental data on the following:

- Performance of high flow-rate spray or jet nozzles using hydrocarbons as the working fluid
- Mean droplet size and droplet size distribution from high flow-rate water spray nozzles
- Vertical fluid projection limits of any nozzle operating at the pressure and flow-rates required for a 1-KT simulation

In Section 6.2 serious doubt was cast upon the ability of a spray nozzle to project to a height of 140 feet. The results cannot be considered conclusive, however, as no consideration was taken of the influence of the liquid flow-induced motion of the surrounding atmosphere.

Although it is highly desirable from both a cost and safety standpoint to test the dispersal system using water, such a test may have little bearing on the performance of the system using a hydrocarbon. As seen in Section 6.1, several manufacturers indicate that although it may be possible to estimate hydrocarbon performance using water, this procedure does not always lead to the correct results. To have a high confidence in nozzle performance, candidate nozzles must be tested with candidate fuels.

SECTION 7

COMPARISON OF CANDIDATE FUELS

Successful weaponization of the FAE concept has been obtained using ethylene oxide as fuel (Reference 10). This material has a clear military advantage over many of the hydrocarbon fuels in that it is water-soluble which reduces the fire hazard in the event of a spill, particularly on-board ship. It has a high density and its detonation limits do not vary significantly over very large ranges in ambient temperature. Such considerations are not necessarily pertinent to FAE used as a simulation device and other fuels were investigated.

Confined detonations have been observed in such diverse materials as kerosene, diethylcyclohexane, decane, hexadecane, and MAPP. NWC has reported unconfined detonations in a great many materials (Reference 12), a sample of which is listed in Table 4. It will be noted that toluene can be detonated if the liquid is preheated, but it cannot support a detonation if the vapor is initially cold. Methane cannot be detonated in air and the only data on kerosene is the laboratory, confined-detonation work of the University of Michigan (Reference 21). Although we have entered a "?" for the unconfined detonation of acetylene, it is well known that this material can support a detonation over very wide concentration limits (Reference 28).

The bulk costs of the fuels were obtained by directly contacting various suppliers. Many of the more common fuels, such

TABLE 4 COMPARISONS OF CANDIDATE FUELS

Candidate Fuel	Unconfined Detonation	Bulk Cost		Toxic Hazard*
		\$/ton	\$/10 ⁹ cal	
Ethylene Oxide	Yes (NWC)	2500	395	3/2
Propylene Oxide	Yes (NWC)	1160	170	2/2
Ethylene	?	1940	180	0/2
Acetylene	?	1500	135	0/2
MAPP	Yes (AFATL)	600	85	0/0
Toluene	Yes-Warm (NWC) No-Cold (NWC)	1860	200	1/2
Diethylether	Yes (NWC)	720	90	2/2
Propylnitrate	Yes (Northrup)	2500		
Methane (LNG)	No (NWC)	1365	115	0/1
Propane (LPG)	Yes (NWC)	255	24	0/1
Butane	Yes (NWC)	115	12	0/2
Hexane	Yes (NWC)	160	15	1/1
Heptane	?	140	13	1/2
Gasolene	Yes (NWC)	115	11	2/2
Kerosene	? Lab (UM)	124	13	1/2
Diesel Fuel	?	102	11	1/2

* See text for definitions of hazard numbers

as gasoline, propane, and diesel fuel, can be obtained in tank car quantities while the more exotic fuels such as ethylene oxide, diethylether, etc., can only be obtained in 55 gallon drums or smaller. Ethylene oxide is unique, in that it is shipped only in reinforced canisters, each of which require a substantial monetary deposit (in excess of \$400). The bulk costs for the fuels enumerated in Table 4 do not include any canister deposits. The costs are the quotations from the suppliers, valid as of March 1977, and reflect their prices for the largest quantities that can be shipped. The second column, under the heading of bulk cost, is the cost per unit explosive yield measured in TNT equivalent tons. (10^9 calories is the energy output of one metric ton of TNT.)

The toxicity hazard associated with handling the candidate fuels is seen as the last column of Table 4. These data were taken from Reference 29 herein two general groupings of hazards are discussed. They are acute and chronic hazards, the latter being associated with long term (weeks or months) handling of the material. This is not pertinent to our work and has not been incorporated in the table. The acute hazard refers to a one-time or short-term contact with the material. There are two classifications of this hazard, the first being a direct application of the material to the skin, while the second, or internal hazard, would normally be associated with the inhalation of the vapors. A rating of 0 indicates little or no toxicity while the highest rating, 3, indicates that extreme caution is to be used in handling the material. The rating numbers in the toxicity hazard column are read: external/inhalation. Included in the external hazard are frost bite and severe drying of the skin, while the internal hazards include, but are not limited to, lung inflammation, nausea, and

anesthesia (diethylether, "ether," is well known for its anesthetic properties).

High cost and high toxicity make ethylene oxide unattractive as a candidate for the simulation concept. The combination of low cost and relatively low toxicity make the more common fuels, such as propane, butane, and heptane more desirable as candidates. MAPP should also be included, as its detonation properties have been well documented and it has a very high vapor pressure which may insure the formation of a vapor cloud with little or no rain-out of the fuel. Furthermore, MAPP is an unusually safe fuel to handle (Reference 28). The high vapor pressure considerations also apply to propane.

Mixtures of octane and heptane form the standard for the "octane rating" of motor fuels. A gasoline which has the same burning rate as pure octane is said to have an octane rating of 100. The lower the octane rating the higher the detonability of the gasoline. Thus, pure octane would appear to be a poor candidate for a FAE, while heptane, being a more easily detonated fuel, would appear to be a good candidate. Heptane has thus been included in our list of candidate fuels, although it has been subjected to little FAE experimentation. It should be noted, however, that the boiling point of heptane is 98.4°C. This may make its dispersion more difficult than that of MAPP or propane.

SECTION 8

CONCLUSIONS AND RECOMMENDATIONS

1. Explosively disseminated FAE airblast data show a nuclear surface burst equivalency of 170 tons of fuel per kiloton for fuel clouds having a height-to-diameter ratio of 0.2.
2. The errors associated with predicting airblast parameters from explosively disseminated fuel clouds are approximately three times those associated with condensed explosive nuclear-airblast simulation experiments.
3. The use of detonation points offset from the center of the FAE cloud causes multiple airblast shocks which contribute to azimuthal variations in airblast parameters. Multiple shocks would be undesirable in a nuclear-airblast simulation.
4. Although hemispherical balloons filled with fuel-air mixtures show nuclear surface burst equivalencies of 63- to 88-tons of fuel per kiloton, the fuel vapor was well mixed with air (or oxygen) over very long times (in comparison with simulation fuel dissemination times) and consequently the data are believed unrealistically low for unconfined aerosol fuel clouds disseminated within a few seconds.
5. A realistic estimate of the nuclear surface burst equivalencies of unconfined aerosol fuel clouds is believed to be 150 tons of fuel per kiloton for clouds in a cylindrical geometry for a height-to-diameter ratio of approximately 0.2.
6. Vapor/aerosol-air mixtures, for a 1-KT simulation, require cloud dimensions of gigantic proportions, approximately 140 feet high and 700 feet in diameter. These large cloud dimensions require multiple fuel dispersion points and place great emphasis on fuel dispersion techniques.
7. Increasing the height-to-diameter ratio of the cylindrical fuel cloud increases the overpressure-impulse effectiveness of the FAE. However, this is offset by requirements for larger fuel dissemination heights with a consequent greater dependency on ambient wind velocities.

8. Aerosols with mean droplet diameters less than 2500 microns will support detonation. The smaller the droplet diameter, the closer the detonation will be to the ideal Chapman-Jouget shock conditions for the vapor.
9. Detonations will be supported for fuel concentration with a factor of 1.5 on each side of the stoichiometric mixture.
10. Spray nozzles exist with performance characteristics in the flow rates necessary for a 1-KT simulation but very little information exists on droplet size distribution and/or vertical reach for these nozzles.
11. Theoretical estimates of the maximum vertical reach of single droplets indicate that the necessary cloud heights may not be possible for spray nozzles producing droplets of 1500 microns or less.
12. Performance of nozzles using other than water as a working fluid must be evaluated using the candidate nozzle and the candidate fuel.
13. High cost and high toxic hazard make ethylene oxide a poor candidate for FAE nuclear-airblast simulation experiments.
14. Low cost and low toxicity hazards point toward propane, MAPP, and butane as being the attractive candidate fuels for FAE nuclear-airblast simulation experiments with heptane being worthy of consideration.

REFERENCES

1. S.F. Fields and L.E. Fugelson, "Blast Simulation with Balloons Containing Detonable Gas," DNA 3432F, December (1974).
2. L.E. Perkins, "BADM-1 Static Warhead Tests," Naval Weapons Center, China Lake, CA., Memorandum for the Record 4563-109-76, 20 October (1975).
3. Anon. "A New Simulation Facility for Atomic Explosions, (Project FAX), Phase I. Preliminary Engineering Feasibility," MSA-FCR-13-DNA, McMillan Science Associates, Inc., Los Angeles, CA. August (1975), (draft).
4. F. J. Klima, J. M. Balcerzak, and M. R. Johnson, "High Altitude Blast Generation System, Part I, Theoretical and Experimental Analysis," DASA 2303-I, December (1967).
5. R. B. Morrison and R. W. Oliver, "A New Simulation Facility for Atomic Explosions, (Project FAX), Phase II. Definition and Design of Experimental Facility," McMillan Scientific Associates, Inc., Los Angeles, CA. October (1976), (draft).
6. P. A. Ellis, D. C. Sachs, and P. J. Morris, "Nuclear Weapons Blast Phenomena, Volume 11, Blast Wave Interactions (U)," DASA 1200-II, December (1970), (C-RD).
7. R. E. Reisler, USA Ballistic Research Laboratories, Aberdeen Proving Ground, Md. (Private Communication).
8. G. D. Teel, "Free Field Experiment, Pre-Mine Throw IV," POR-6830, Ballistic Research Laboratories, Aberdeen Proving Ground, Md., August (1975).
9. M. M. Swisdak, "Explosion Effects and Properties, Part I- Explosion Effects in Air," NSWC/WOL/TR75-116, October (1975).
10. L. E. Perkins, "Analysis of 300 Pound and 1000 Pound FAE Data," Naval Weapons Center, China Lake, CA. Memorandum for the Record, 24 October (1972).

11. J. A. Dennis, "Report of Variable Parameters on the Blast Effects of Navy BLU-73/Fuel Air FAE Warheads (U)," MERDC Report No. 2071, August (1973), (C).
12. J. Bowen, Naval Weapons Center, China Lake, CA., Private Communication.
13. L. Perkins, "Fuel-Air Explosive (FAE) Height-of-Burst Tests," MWC Technical Memorandum 2633, Naval Weapons Center, China Lake, CA., December (1975).
14. H.D. Nation, "Measurement and Analysis of Hemispherical Fuel-Air Explosives (FAE) (U)," ADTC-TR-76-109, December (1976), (C).
15. R. T. Sedgwick, H. R. Kratz, and M. Baker, "Concepts for Improved Fuel-Air-Explosives," Systems, Science and Software, La Jolla, CA., SSS-R-77-3305, September (1976).
16. J. R. Bowen, K. W. Ragland, F. J. Stevens, and T. F. Loflen, "Heterogeneous Detonation Supported by Fuel Fogs or Films," Thirteenth Symposium (International) on Combustion, The Combustion Institute, Pittsburgh, PA (1971), pp. 1131-1139.
17. E. K. Dabora, K. W. Ragland, and J. A. Nicholls, "Drop Size Effects in Spray Detonations," Twelfth Symposium (International) on Combustion, The Combustion Institute, Pittsburgh, PA., (1969), pp. 19-26.
18. R. S. Fray and J. A. Nicholls, "Blast Imitation and Propagation of Cylindrical Detonations in MAPP-Air Mixtures," AIAA Journal, 12, 12, 1703-1708 (1974).
19. C. W. Kaufman and J. A. Nicholls, "Shock Wave Initiation of Liquid Fuel Drops," AIAA Journal, 9, 5, 880-885 (1971).
20. A. K. Oppenheim and R. I. Soloukhin, "Experiments in Gas Dynamics of Explosion," Ann. Rev. Fluid Mech. 5, 31-58 (1973).
21. J. A. Nicholls, M. Sichel, R. Fry, and D. R. Glass, "Theoretical and Experimental Study of Cylindrical Shock and Heterogeneous Detonation Waves," Acta Astronautica 1, 385-405 (1974).
22. Bete Fog Nozzle, Inc., "Bete Fog Nozzles," Catalog No. 76.

23. Hulick, Private Communication, Research Department, Monarch Manufacturing Works, Inc., 2505 East Ontario Street, Philadelphia, PA.
24. Delavan Manufacturing Company, "Delavan Industrial Nozzles and Accessories," Catalog No. 1622-177.
25. Spraying Systems Company, "Spray Nozzles and Accessories," Industrial Catalog 26A and Supplemental Data Sheets.
26. W. G. Labes, "Evaluation of Fire Protection Spray Devices State of the Art," National Bureau of Standards Report, NBS-GCR-76-72, June 30 (1976).
27. Handbook of Chemistry and Physics, Chemical Rubber Publishing Company, Cleveland, Ohio; 33rd edition.
28. Anon. "MAPP Gas--The Safe High-Energy Fuel," MAPP Products, PO Box 105, Diamond Road, Springfield, New Jersey, Brochure ADG-MAPP-1013.
29. N. I. Sax, Dangerous Properties of Industrial Materials, Van Nostrand-Rhineholt Company, 4th Edition (1975).